Time-dependent Adjoint-based Optimization for Coupled Fluid-Structure Problems

Asitav Mishra, Post-doctoral scholar, University of Michigan

Dimitri Mavriplis, Professor, University of Wyoming
Jay Sitaraman, Research Scientist, Parallel Geometrics LLC
(Karthik Duraisamy, Associate Professor, University of Michigan)

Outline

- Introduction
- Background
- Motivation & Objective
- Coupled CFD/CSD Analysis, Sensitivity and Adjoint
  - Hart-II blade optimization in Hover/Cruise
  - Hart-II multi-point (hover+cruise) optimization
- Conclusion

Introduction

- Helicopter flight envelope expansion
- Optimized blade design
- Adjoint optimization
- Helicopter rotor blade design: a *coupled* aero/ structure problem
- Need of *aero-structural* coupled adjoint optimization

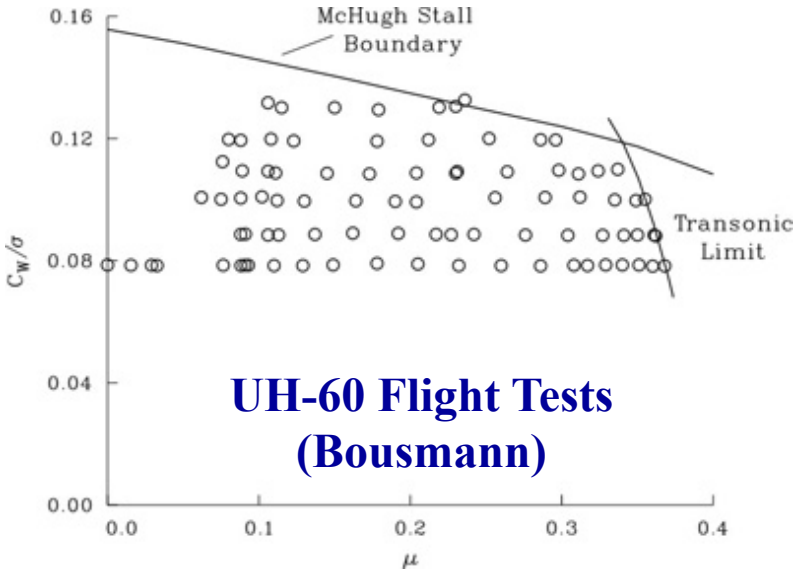

UH-60 Flight Tests (Bousmann)

Mi-26

Background

- Adjoint optimization: computational cost independent of number of design variables
  - Steady: fixed wing shape optimizations
  - Unsteady: Mavriplis, Mani, Nielsen
  - Helicopter blade design
    - Hover: Mani, Lee
    - Forward flight: Nielsen, Choi, Alonso

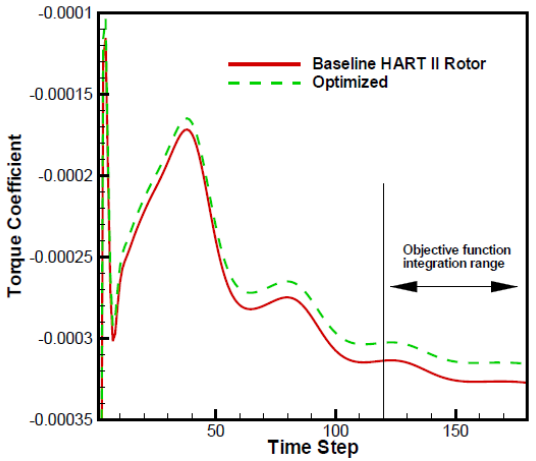

Mani (AIAA 2013)

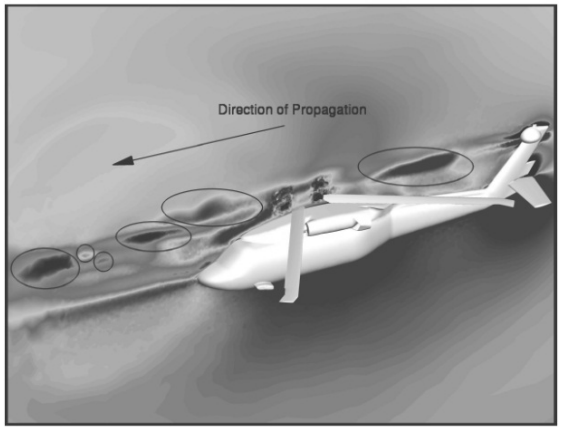

Nielsen (AIAAJ 2013)

Motivation & Objective

- Limited *structural* adjoint optimization of rotor blade design
- Limited *coupled* fluid structure optimization
- Objective
  - Develop strongly coupled CFD/CSD *analysis* framework for rotor in hover/forward flight
  - Develop strongly coupled CFD/CSD *adjoint* optimization framework for rotor design
  - Incorporate rotor trim into optimization

Multidisciplinary Problems: Time-Dependent Aeroelasticity

- Fully coupled problem involves 4 modules:
  - Flow solver
  - Structural Solver
  - Mesh deformation
  - Fluid-structure interface (FSI)
- Adjoint formulation leads to :
  - Disciplinary adjoints: Fluids, Structures, Mesh, FSI
  - Disciplinary adjoints are coupled at each time step
  - Coupled adjoint solver analogous (transpose) of coupled aeroelastic analysis solver
  - Demonstrated flutter suppression through shape optimization in 2D
    - Mani and Mavriplis AIAA 2008-6242

Aerodynamic Solver: NSU3D

- 3D unstructured mesh finite-volume RANS solver
- 2nd –order accurate in space and time.
- One equation Spalart-Allmaras turbulence model.
- Deforming mesh capability with GCL compliance
- Fully implicit discretization solved using Newton's method at each time-step as:

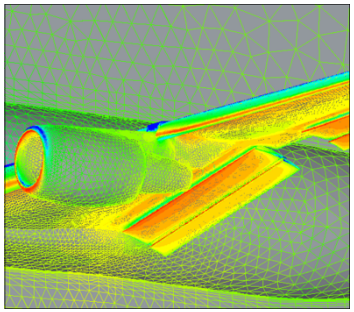

$$\mathbf{R}^n = A\frac{\partial \mathbf{U}}{\partial t} + \mathbf{S}(\mathbf{x}^n, \dot{\mathbf{x}}^n, \mathbf{U}^n) = 0$$

$$\left[\frac{\partial \mathbf{R}(\mathbf{U}^k)}{\partial \mathbf{U}^k}\right] \delta \mathbf{U}^k = -\mathbf{R}(\mathbf{U}^k)$$

$$\mathbf{U}^{k+1} = \mathbf{U}^k + \delta \mathbf{U}^k$$

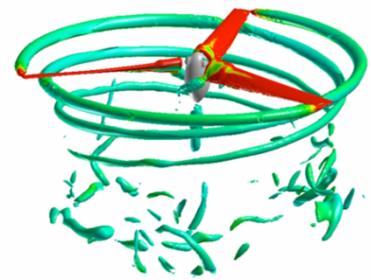

  - Preconditioned GMRES used for linear system
    - Forward linearization used for exact Jacobian-vector products
  - Linear agglomeration multigrid for preconditioner
  - Line implicit solver as smoother for linear multigrid

Structural Analysis: Beam Model

- Hodges-Dowell type finite element based solver
- 15 degrees of freedom (flap, lag, axial and torsion)
- First order system: $\mathbf{Q} = [\mathbf{q}, \dot{\mathbf{q}}]^T$

  where, $\mathbf{J} = [I]\,\dot{\mathbf{Q}} + [A]\,\mathbf{Q} - \mathbf{F} = 0$
- **J** = Residual of structural equation
- **q** = blade dof (displacements)
- **F** = beam (aero) forcing
- **Solved via direct inversion**

Beam FEM model

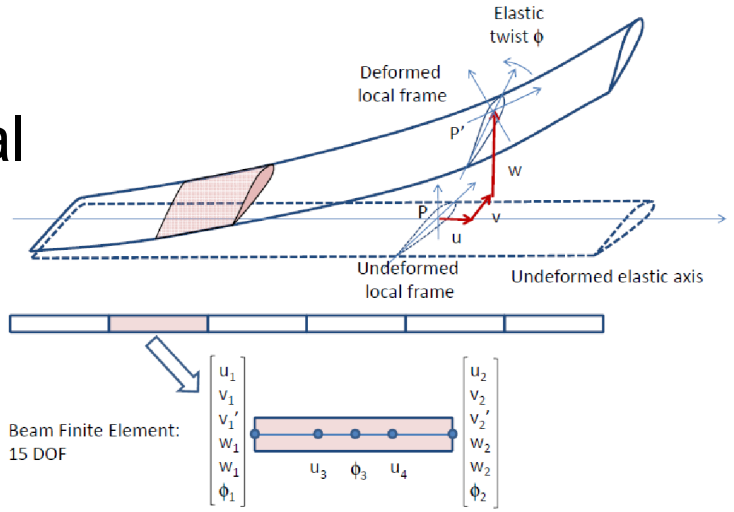

Comparison of Hart-II Natural Frequencies

Modes	Present Model	UMARC	DLR
Flap 1	1.104	1.112	1.125
Flap 2	2.802	2.843	2.835
Flap 3	5.010	5.189	5.168
Torsion 1	3.878	3.844	3.845

Mishra (AIAA Aviation 2013)

Mesh Deformation

- Propagates surface displacements to interior mesh
  - Deflections from structural model at each time step (x^n)
  - Design shape changes (D)
- Based on linear elasticity analogy
  - (more robust than spring analogy)
- Solved using line-implicit agglomeration multigrid (analogous to flow solver)

$$G(x^n, x^n_{surf}, D) = 0$$

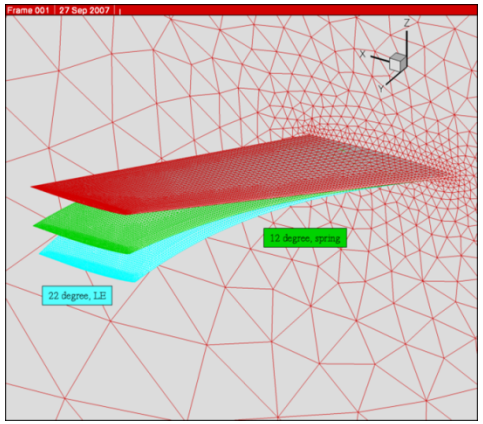

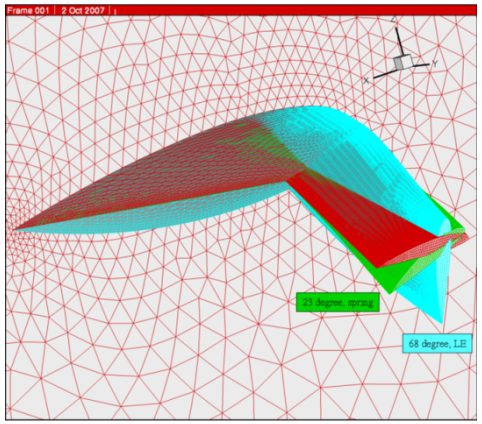

Fluid-Structure Interface (FSI)

- Cloud of surface points associated with beam element
- Forces projected onto beam element shape functions

$$F_{beam} = [T(Q)]F_{cfd}(x,u) \qquad S(F_{beam}, Q, F_{cfd}(x,u)) = 0$$

- Displacements projected back to CFD surface points using transpose

$$x_{surf} = [T(Q)]^T Q$$

$$S'(x_{surf}, Q) = 0$$

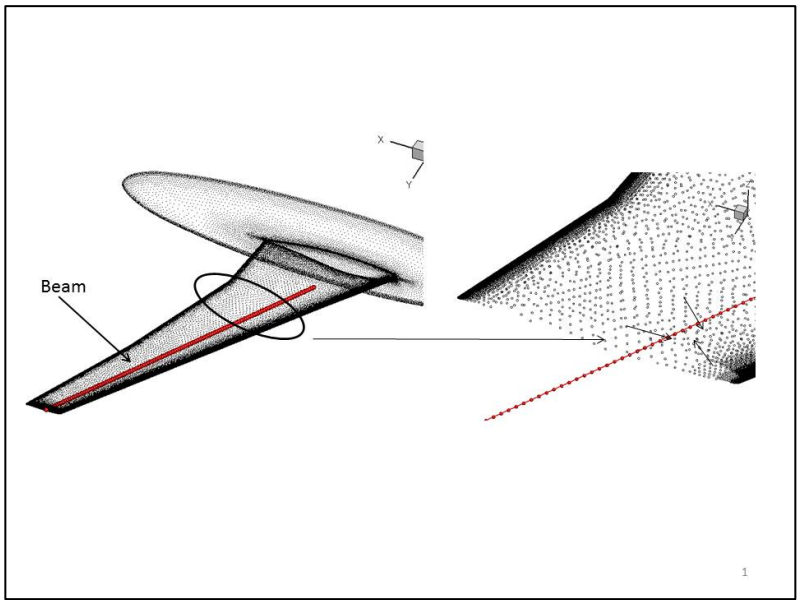

CFD/CSD Coupling Time Integration Methodology

- **Outer loop over physical time steps**
  - **Coupling iterations per time step :**
    - Mesh:
      - Line implicit multigrid
    - Flow:
      - Implicit BDF2 Newton iterations (GMRES)
      - Linear agglomeration multi-grid
    - FSI (Fluid to structure)
      - Explicit assignment
    - Structure:
      - Implicit BDF2 newton iteration (direct inversion)
    - FSI (Structure to fluid)
      - Explicit assignment

Hover (Unsteady) Test Problem

- 4 bladed Hart-II rotor in hover:
  - Rigid & Flexible; M_{tip} = 0.64; 1040 RPM
- CFD/CSD specifications:
  - 2.32 & 11.4 million grid nodes (prisms, pyramids, tets)
  - 20 beam elements
- Tight CFD/CSD coupling
  - 10 rotor revs
  - 2.32M : dt=2^{O}, 1^{O}, 0.5^{O}
    - 6 coupling per time step, **10** CFD and 20 CSD non-linear iterations per coupling
    - ~1 hr/rev with 512 cores
  - 11.4M: dt = 2^{O}
    - 6 coupling per time step, **25** CFD and 20 CSD non-linear iterations per coupling
    - ~2.5 hr/rev with 2048 cores

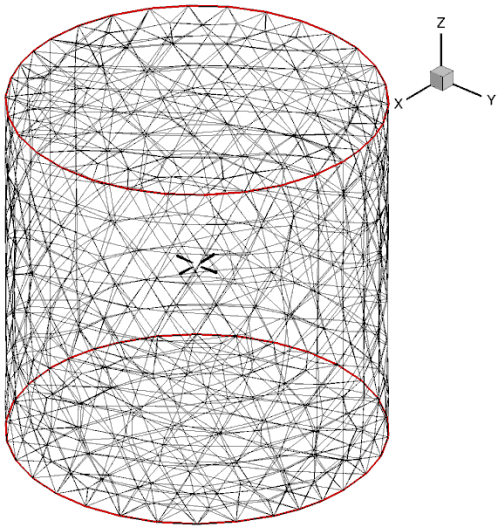

CFD flow domain

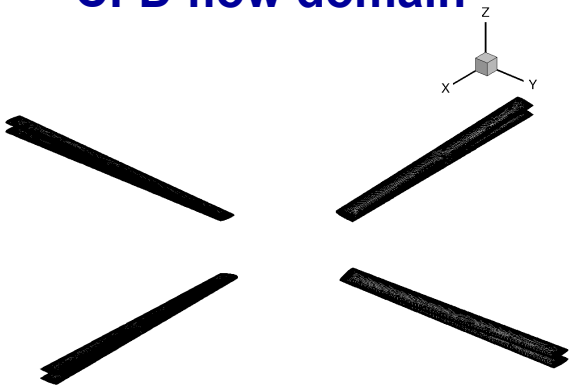

Rigid and Flexible blades

Hover: Analysis Convergence

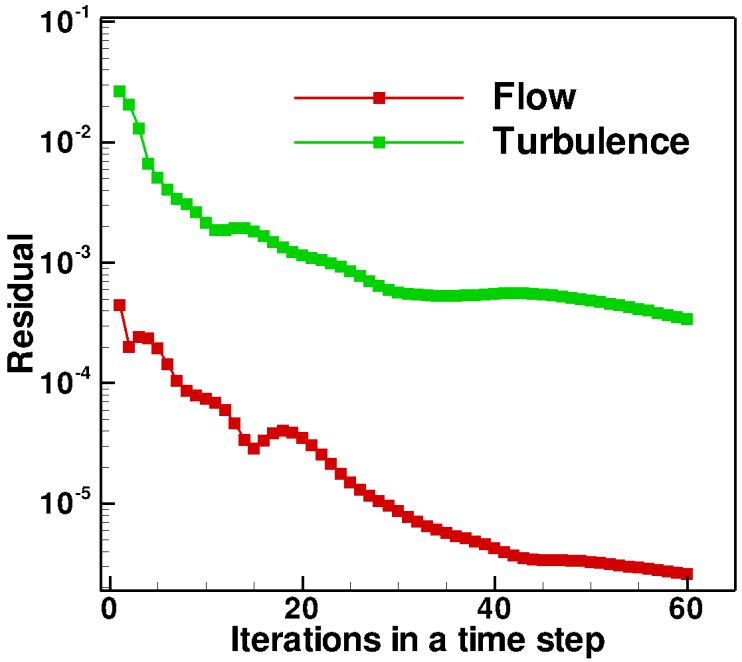

Rigid blade convergence

- 60 non-linear iterations per time step
- 3 multigrid cycles/iteration
- Convergence by 2 orders of magnitude

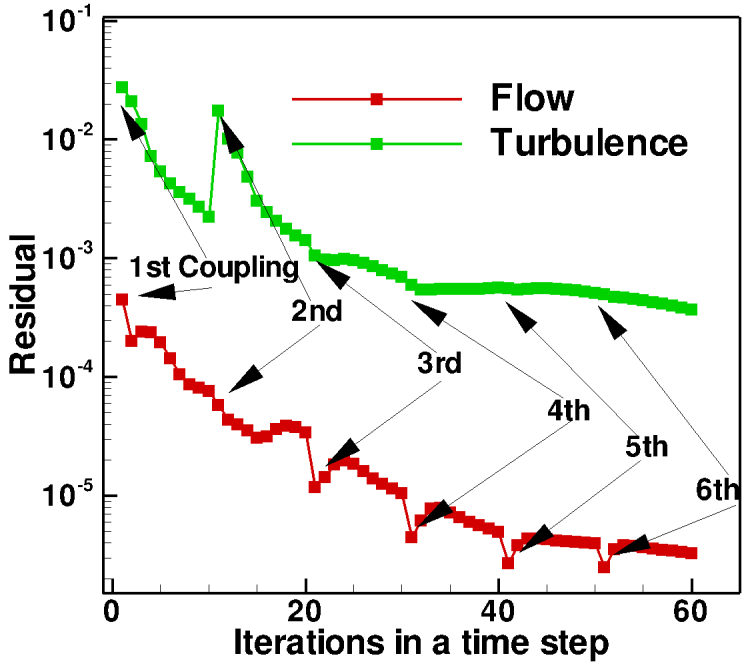

Flexible blade convergence

- 6 coupling cycles per time step
- 10 non-linear iterations/coupling with 3 multi-grid cycles/iteration
- Convergence by 2 orders of magnitude

Hover: Convergence continued…

Mesh convergence per time step

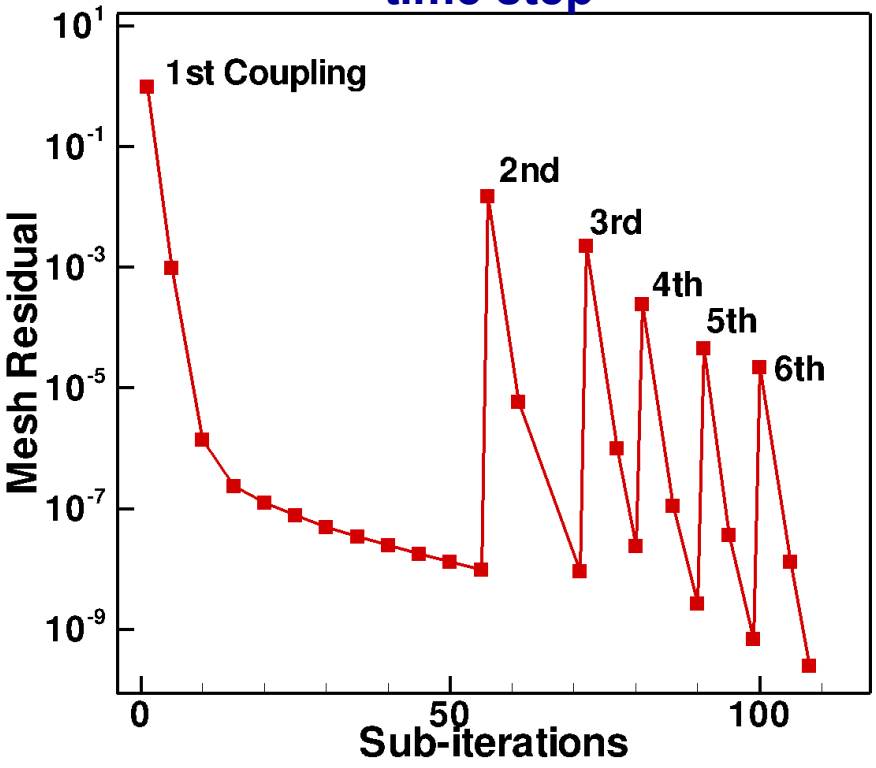

CSD convergence per coupling per time step

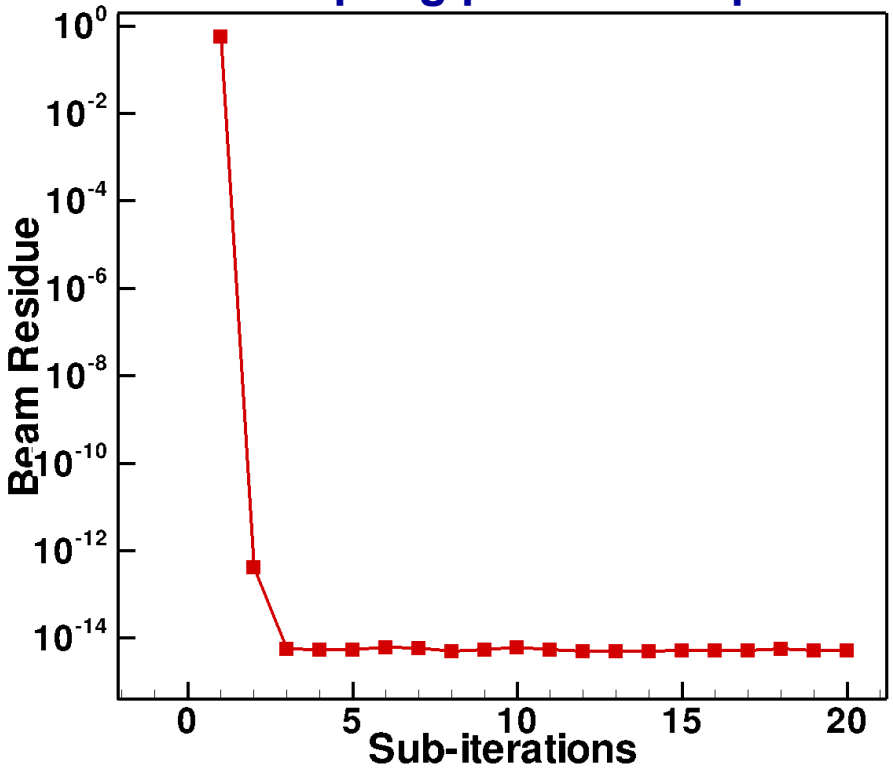

- Mesh solves upto 60 iterations or $1x10^{-9}$ (whichever earlier) per coupling
- Mesh convergence by 10 orders of magnitude per time step (6 coupling cycles)
- Beam convergence to machine precision (faster convergence)

Hover: Blade Tip Time History

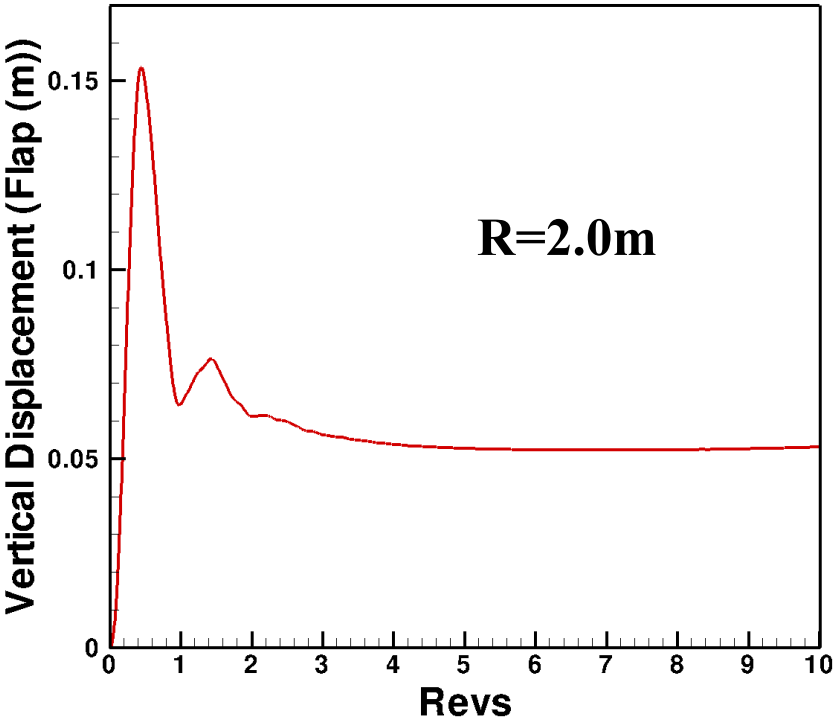

Blade tip vs time

Surface Cp

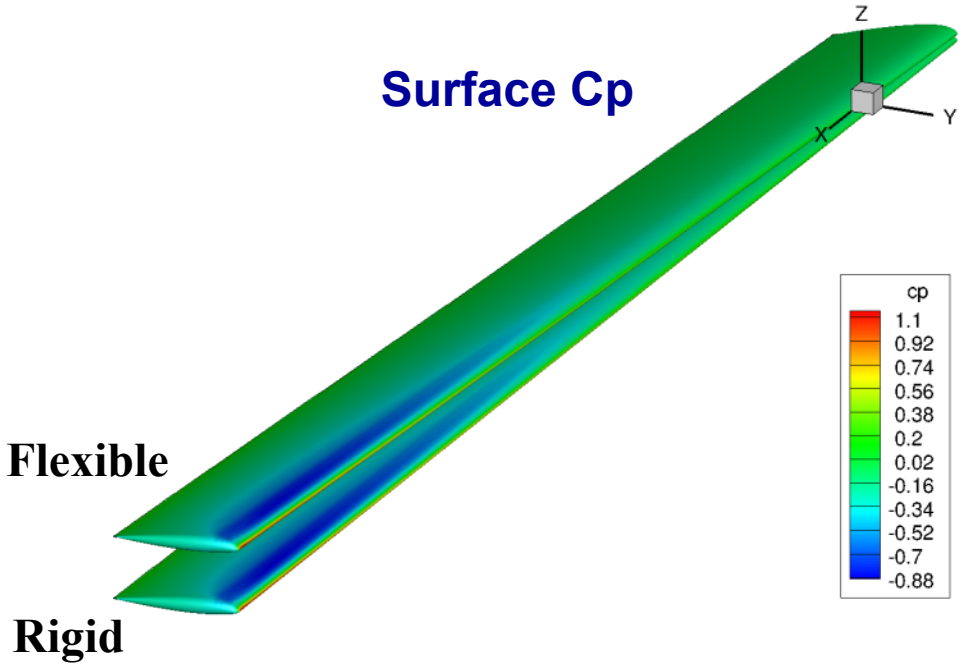

Blade flap over time

- Blade flaps to high values, but converges to a lower value after 10 revs

Hover: Hart-II Performance Prediction

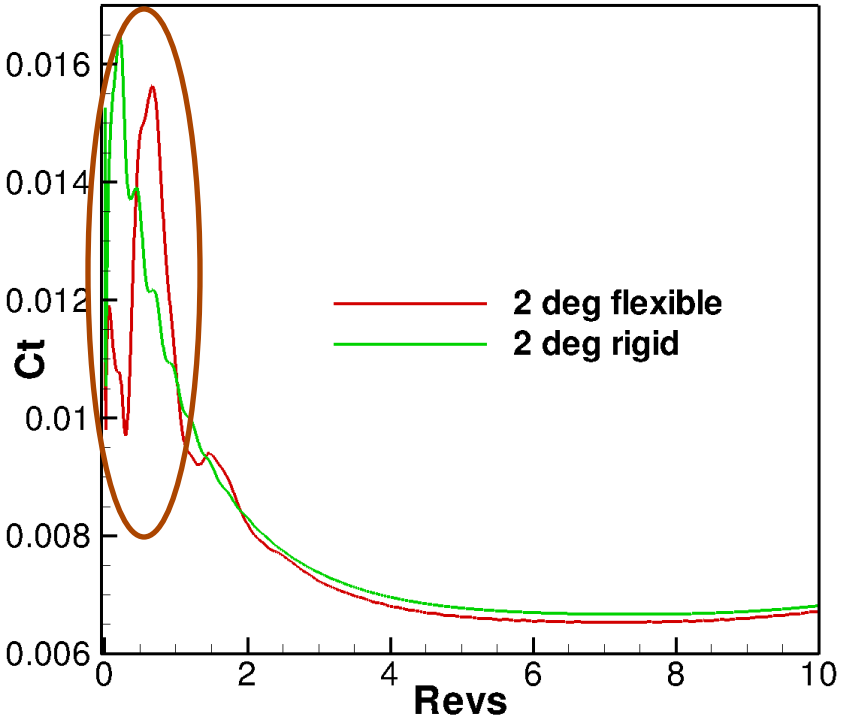

Thrust vs time

Mishra (JCP 2015)

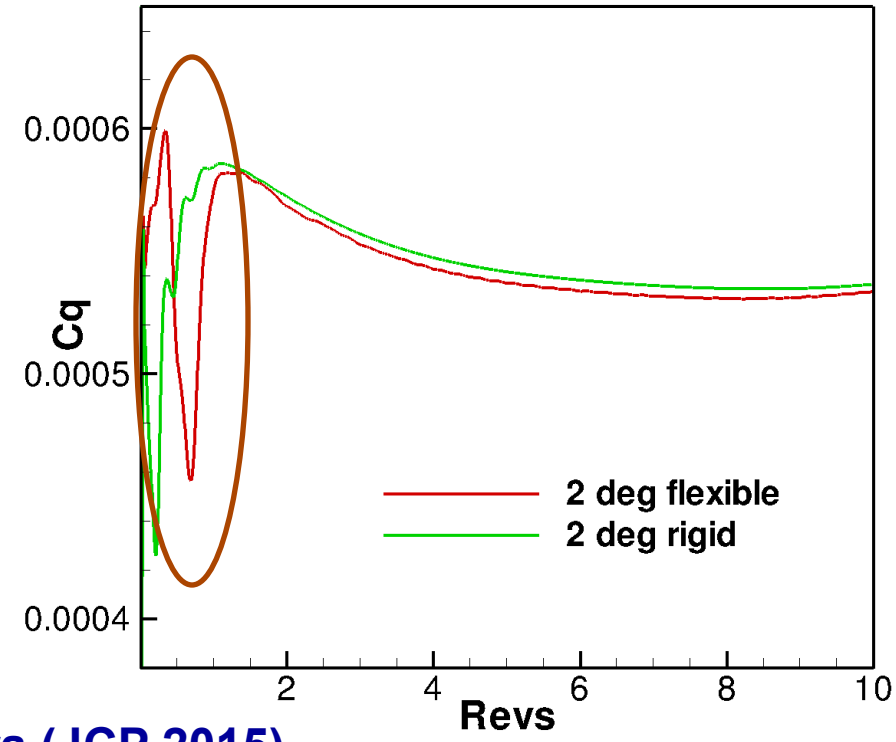

Power vs time

- Focus on 1st rev where aero-elastic effects are important

Forward Flight or Cruise (Unsteady) Test Problem

- 4 bladed Hart-II rotor in forward flight:
  - Rigid & Flexible; M_{tip} = 0.64; 1040 RPM; μ=0.15 (M_∞~0.1); α=5.4^O
- CFD/CSD specifications:
  - 2.32 million grid nodes (prisms, pyramids, tets)
  - 20 beam elements per blade
- Tight CFD/CSD coupling
  - 5 rotor revs
  - 2.32M : $\Delta t = 2^O$
    - 6 coupling per time step, **10** CFD and 20 CSD non-linear iterations per coupling
    - ~40 min/rev with 1024 cores
  - Control Inputs:
    - Collective (θ_O)and Cyclics (θ_{1c}, θ_{1s})

$$\theta_{pitch} = \theta_O + \theta_{1c}\cos\psi + \theta_{1s}\sin\psi$$

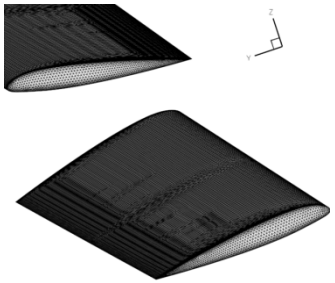

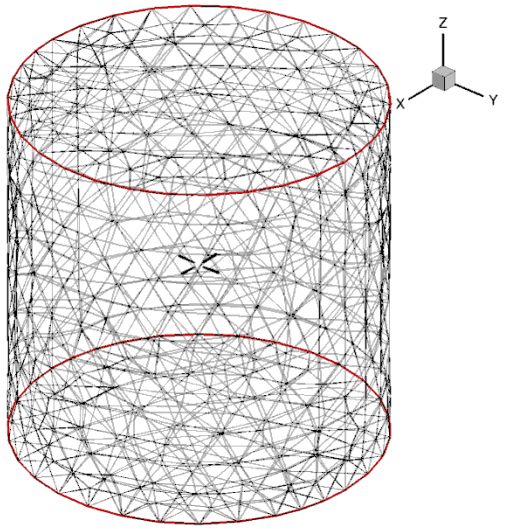

CFD flow domain

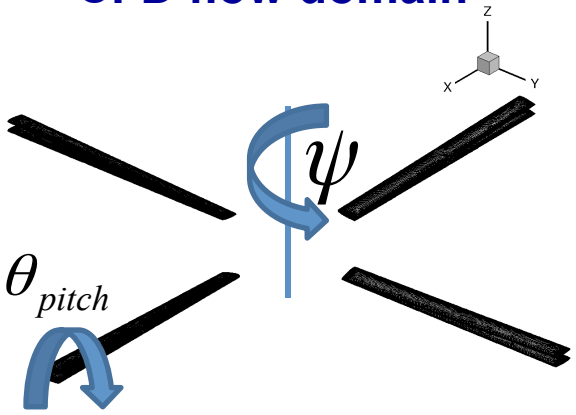

Rigid and Flexible blades

Cruise: Analysis Convergence

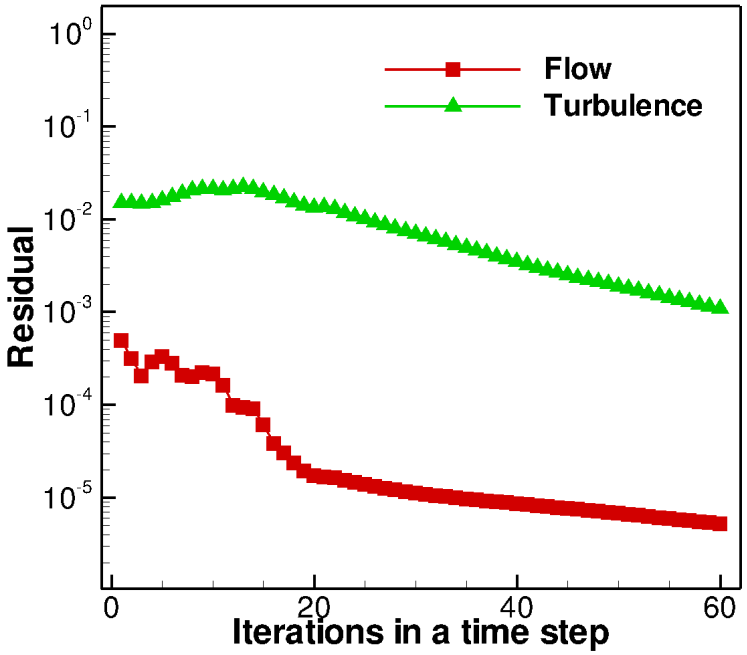

Rigid blade convergence

- 60 non-linear iterations per time step
- 3 multigrid cycles/iteration
- Convergence by 2 orders of magnitude

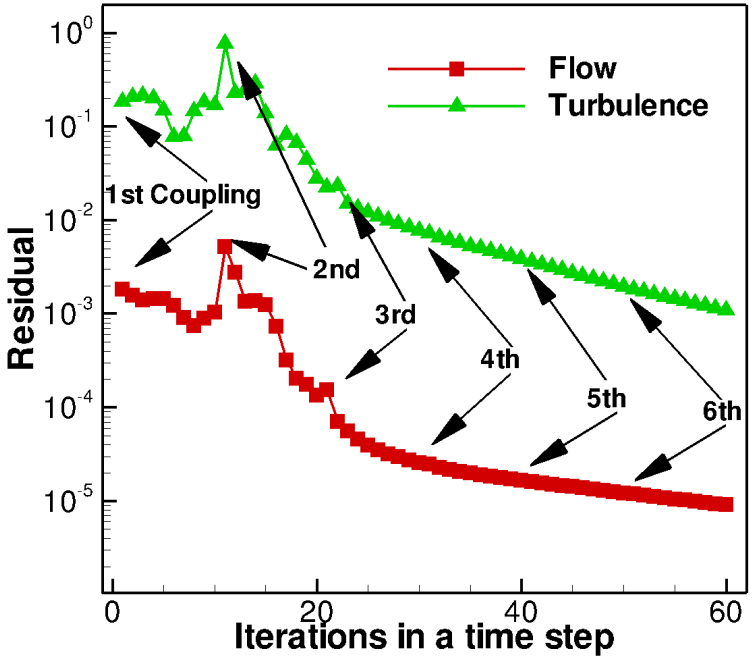

Flexible blade convergence

- 6 coupling cycles per time step
- 10 non-linear iterations/coupling with 3 multi-grid cycles/iteration
- Convergence by 2 orders of magnitude

Cruise: Convergence continued…

Mesh convergence per time step

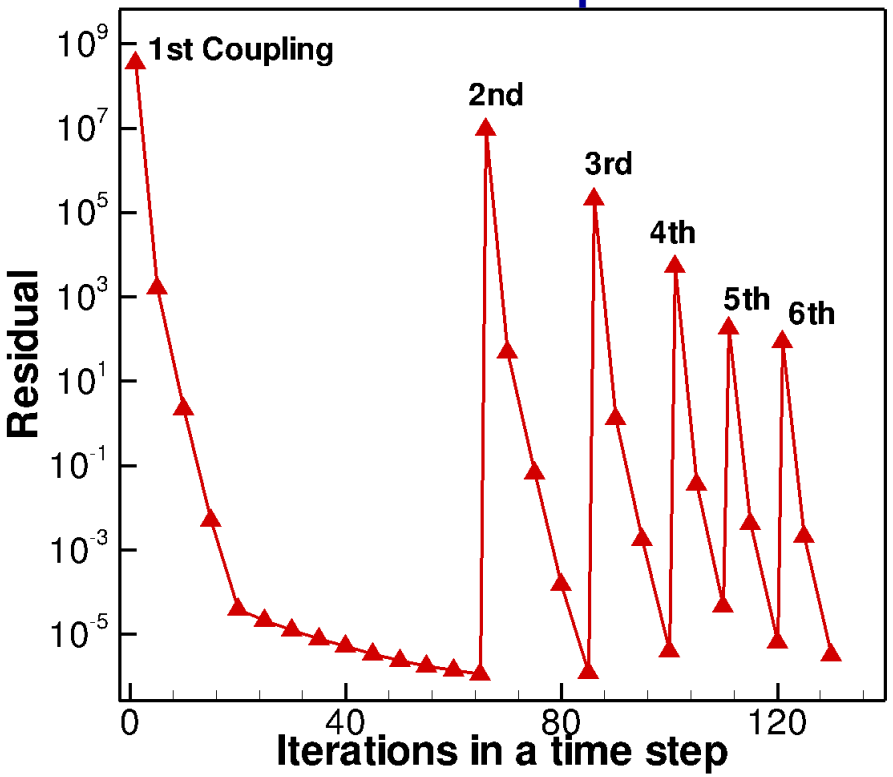

CSD convergence per coupling per time step

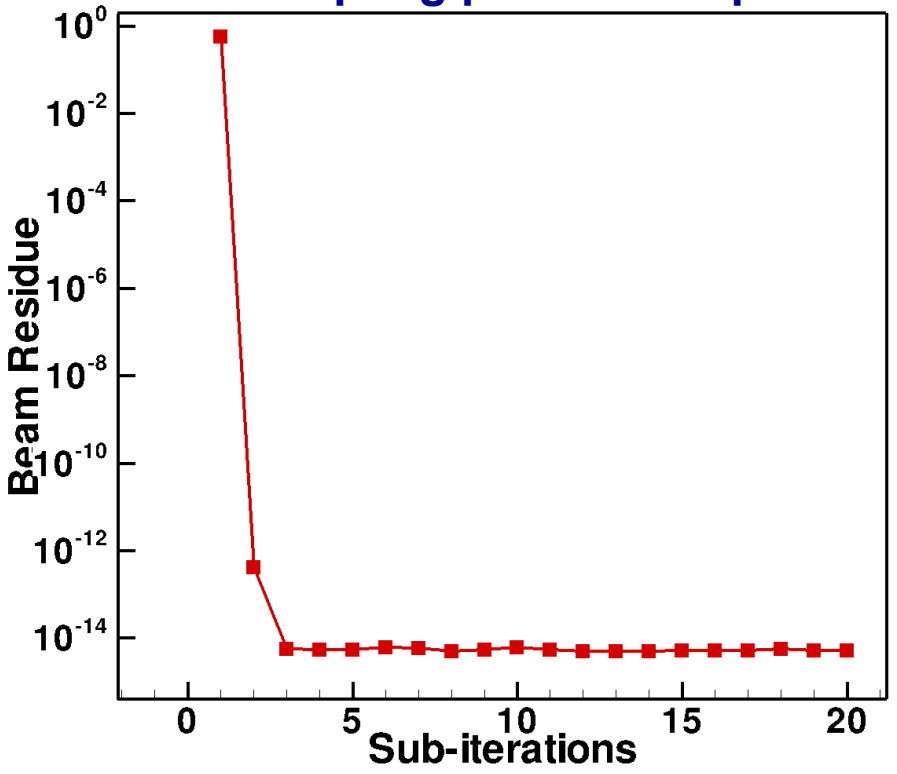

- Mesh solves upto 80 iterations or 1×10^{-9} (whichever earlier) per coupling
- Mesh convergence by 14 orders of magnitude per time step (6 coupling cycles)
- Beam convergence to machine precision (faster convergence)

Cruise: Blade Tip Time History

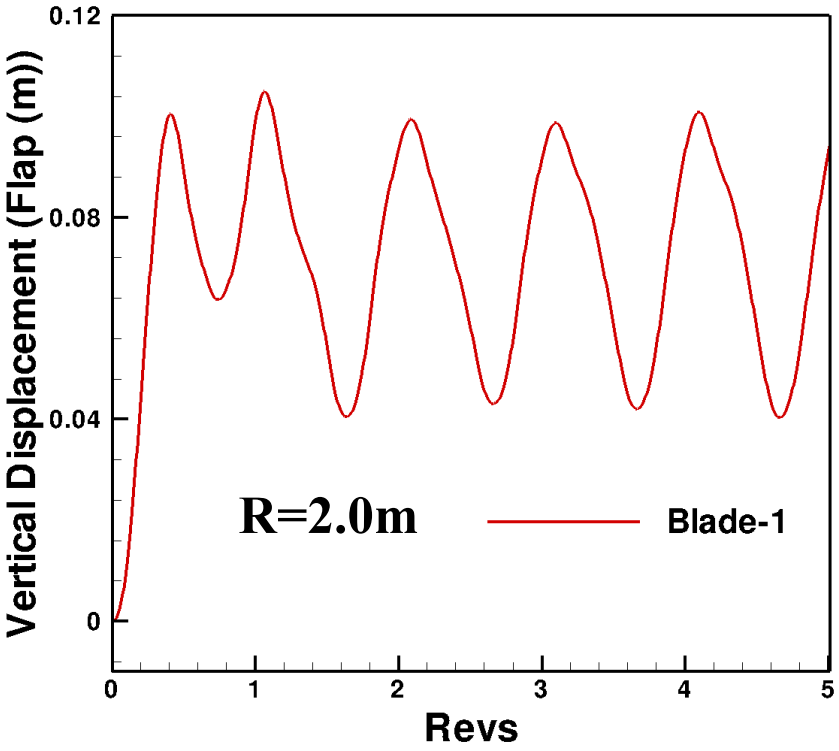

Blade tip vs time

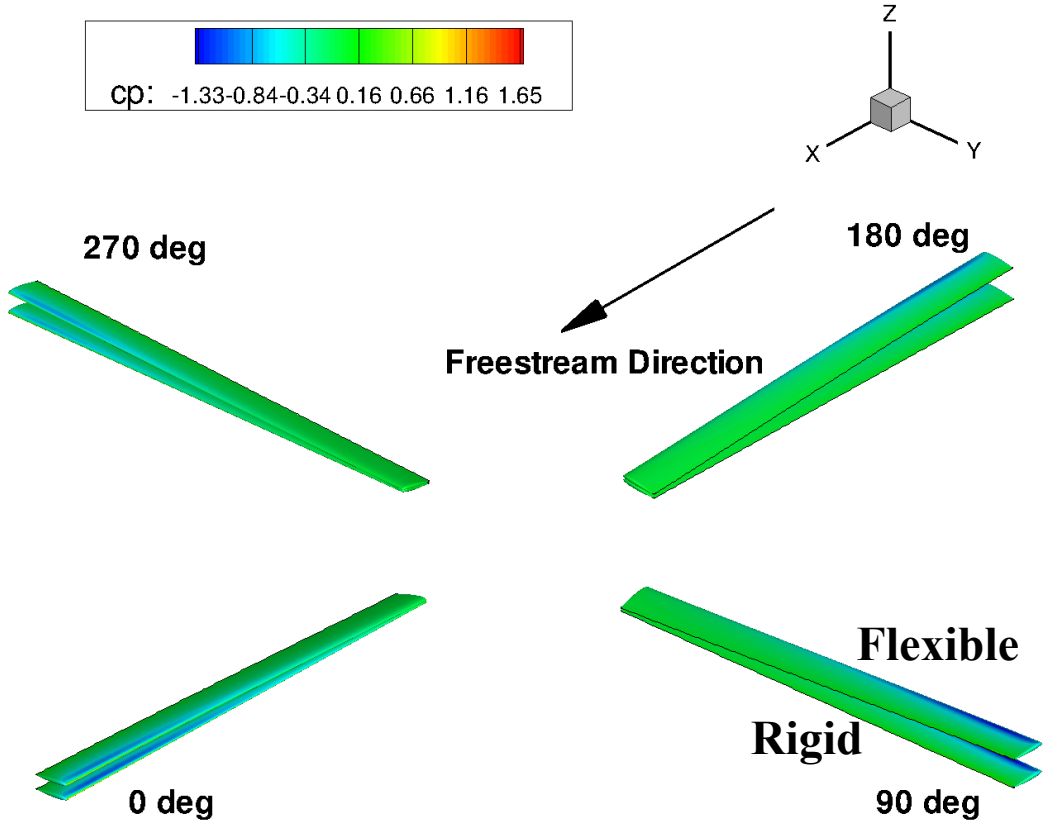

Surface Cp

- Blade flaps to high values, but converges to a lower value after 2 revs

Mishra (AIAAJ 2016)

Discrete Adjoint Formulation (a simplified view)

- Objective: $L = L(D, u(D))$
- Subject to: $R(u(D), D) = 0$
  - R = 0 : flow solution converged
  - u : flow variables (solution)
  - D: design parameters (shape parameters)
- Sensitivities: $\frac{dL}{dD} = \frac{\partial L}{\partial D} + \frac{\partial L}{\partial u}\frac{\partial u}{\partial D}$

- Constraint sensitivity eqn: $\left[\frac{\partial R}{\partial u}\right]\frac{\partial u}{\partial D} + \frac{\partial R}{\partial D} = 0 \quad \left[\frac{\partial R}{\partial u}\right]\frac{\partial u}{\partial D} = -\frac{\partial R}{\partial D}$
- Final form: $\frac{dL}{dD} = \frac{\partial L}{\partial D} - \frac{\partial L}{\partial u}\left[\frac{\partial R}{\partial u}\right]^{-1}\frac{\partial R}{\partial D}$

Discrete Adjoint Formulation

- Sensitivity equation:

$$\frac{dL}{dD} = \frac{\partial L}{\partial D} - \frac{\partial L}{\partial u}\left[\frac{\partial R}{\partial u}\right]^{-1}\frac{\partial R}{\partial D}$$

Evaluate first, define as Λ^T

- Adjoint equation:

$$\left[\frac{\partial R}{\partial u}\right]^T \Lambda = -\left[\frac{\partial L}{\partial u}\right]^T$$

  - No dependence on D
  - Dependence on L

- Final form:

$$\frac{dL}{dD} = \frac{\partial L}{\partial D} + \Lambda^T \frac{\partial R}{\partial D}$$

- Cost is independent of number of D's
- dL/dD are then used by a gradient based optimizer to find next best shape

Fully Coupled Fluid-Structure Analysis

Per coupling cycle

- General solution:
- Blade deformation transfer

$$\left[\frac{\partial \mathbf{G}}{\partial \mathbf{x}}\right]\Delta \mathbf{x}^{c} = -\mathbf{G}(\mathbf{x}^{c-1}, \mathbf{x}_s^{c-1})$$

$$\left[\frac{\partial \mathbf{J}}{\partial \mathbf{Q}}\right]\Delta \mathbf{Q}^{c} = [T]^{T}\mathbf{Q}^{c}$$

$$\left[\frac{\partial \mathbf{R}}{\partial \mathbf{u}}\right]\Delta \mathbf{u}^{c} = -\mathbf{R}(\mathbf{u}^{c-1}, \mathbf{x}^{c})$$

Flow:

Transfer:

Structure:

Blade deformation transfer:

$$\mathbf{G}(\mathbf{x}, \mathbf{x}_s(\mathbf{Q})) = \mathbf{0}$$

$$\mathbf{R}(\mathbf{u}, \mathbf{x}) = \mathbf{0}$$

$$\mathbf{S}(\mathbf{F}_b, \mathbf{Q}, \mathbf{F}_{cfd}(\mathbf{x}, \mathbf{u})) = \mathbf{0}$$

$$\mathbf{J}(\mathbf{Q}, \mathbf{F}_b) = \mathbf{0}$$

$$\mathbf{S}'(\mathbf{x}_s, \mathbf{Q}) = \mathbf{0}$$

Fully Coupled Fluid-Structure Sensitivity: Tangent

- Functional sensitivity:

$$\frac{dL}{d\mathbf{D}} = \begin{bmatrix} \frac{\partial L}{\partial \mathbf{x}} & \frac{\partial L}{\partial \mathbf{u}} \end{bmatrix} \begin{bmatrix} \frac{\partial \mathbf{x}}{\partial \mathbf{D}} \\ \frac{\partial \mathbf{u}}{\partial \mathbf{D}} \end{bmatrix}$$

- Solve:

$$\begin{bmatrix} \frac{\partial \mathbf{G}}{\partial \mathbf{x}} & 0 & 0 & 0 & 0 & \frac{\partial \mathbf{G}}{\partial \mathbf{x}_s} \\ \frac{\partial \mathbf{R}}{\partial \mathbf{x}} & \frac{\partial \mathbf{R}}{\partial \mathbf{u}} & 0 & 0 & 0 & 0 \\ -\frac{\partial \mathbf{F}}{\partial \mathbf{x}} & -\frac{\partial \mathbf{F}}{\partial \mathbf{u}} & I & 0 & 0 & 0 \\ 0 & 0 & \frac{\partial \mathbf{S}}{\partial \mathbf{F}} & \frac{\partial \mathbf{S}}{\partial \mathbf{F}_b} & \frac{\partial \mathbf{S}}{\partial \mathbf{Q}} & 0 \\ 0 & 0 & 0 & \frac{\partial \mathbf{J}}{\partial \mathbf{F}_b} & \frac{\partial \mathbf{J}}{\partial \mathbf{Q}} & 0 \\ 0 & 0 & 0 & 0 & \frac{\partial \mathbf{S}'}{\partial \mathbf{Q}} & \frac{\partial \mathbf{S}'}{\partial \mathbf{x}_s} \end{bmatrix} \begin{bmatrix} \frac{\partial \mathbf{x}}{\partial \mathbf{D}} \\ \frac{\partial \mathbf{u}}{\partial \mathbf{D}} \\ \frac{\partial \mathbf{F}}{\partial \mathbf{D}} \\ \frac{\partial \mathbf{F}_b}{\partial \mathbf{D}} \\ \frac{\partial \mathbf{Q}}{\partial \mathbf{D}} \\ \frac{\partial \mathbf{x}_s}{\partial \mathbf{D}} \end{bmatrix} = \begin{bmatrix} -\frac{\partial \mathbf{G}}{\partial \mathbf{D}} \\ 0 \\ 0 \\ 0 \\ 0 \\ 0 \end{bmatrix}$$

Per coupling cycle

Force
Surface
Mesh and
Deformation
Flow
Sensitivity
Structure

$$\begin{bmatrix} \begin{bmatrix} \frac{\partial \mathbf{S}}{\partial \mathbf{F}_b} & \frac{\partial \mathbf{S}}{\partial \mathbf{Q}} \end{bmatrix} \begin{bmatrix} \frac{\partial \mathbf{F}_b}{\partial \mathbf{D}}^c \end{bmatrix} \\ \begin{bmatrix} \frac{\partial \mathbf{J}}{\partial \mathbf{F}_b} & \end{bmatrix} \begin{bmatrix} \frac{\partial \mathbf{x}_s}{\partial \mathbf{D}}^c \end{bmatrix} = -\frac{\partial \mathbf{S}'}{\partial \mathbf{Q}} \frac{\partial \mathbf{Q}}{\partial \mathbf{D}}^c \end{bmatrix} = \begin{bmatrix} -\frac{\partial \mathbf{S}}{\partial \mathbf{F}} \frac{\partial \mathbf{F}}{\partial \mathbf{D}}^c \\ 0 \end{bmatrix}$$

Fully Coupled Fluid-Structure Sensitivity: Adjoint

- Solve:

$$\begin{bmatrix} \frac{\partial \mathbf{G}}{\partial \mathbf{x}}^T & \frac{\partial \mathbf{R}}{\partial \mathbf{x}}^T & -\frac{\partial \mathbf{F}}{\partial \mathbf{x}}^T & 0 & 0 & 0 \\ 0 & \frac{\partial \mathbf{R}}{\partial \mathbf{u}}^T & -\frac{\partial \mathbf{F}}{\partial \mathbf{u}}^T & 0 & 0 & 0 \\ 0 & 0 & I & \frac{\partial \mathbf{S}}{\partial \mathbf{F}}^T & 0 & 0 \\ 0 & 0 & 0 & \frac{\partial \mathbf{S}}{\partial \mathbf{F_b}}^T & \frac{\partial \mathbf{J}}{\partial \mathbf{F_b}}^T & 0 \\ 0 & 0 & 0 & \frac{\partial \mathbf{S}}{\partial \mathbf{Q}}^T & \frac{\partial \mathbf{J}}{\partial \mathbf{Q}}^T & \frac{\partial \mathbf{S'}}{\partial \mathbf{Q}}^T \\ \frac{\partial \mathbf{G}}{\partial \mathbf{x_s}}^T & 0 & 0 & 0 & 0 & \frac{\partial \mathbf{S'}}{\partial \mathbf{x_s}}^T \end{bmatrix} \begin{bmatrix} \Lambda_\mathbf{x} \\ \Lambda_\mathbf{u} \\ \Lambda_\mathbf{F} \\ \Lambda_{\mathbf{F_b}} \\ \Lambda_\mathbf{Q} \\ \Lambda_{\mathbf{x_s}} \end{bmatrix} = \begin{bmatrix} \frac{\partial L}{\partial \mathbf{x}}^T \\ \frac{\partial L}{\partial \mathbf{u}}^T \\ 0 \\ 0 \\ 0 \\ 0 \end{bmatrix}$$

Per coupling cycle

$$\begin{bmatrix} \frac{\partial \mathbf{G}}{\partial \mathbf{x}}^T & \frac{\partial \mathbf{R}}{\partial \mathbf{x}}^T \\ 0 & \frac{\partial \mathbf{R}}{\partial \mathbf{u}}^T \end{bmatrix} \begin{bmatrix} \Lambda_\mathbf{x}{}^c \\ \Lambda_\mathbf{u}{}^c \end{bmatrix} = \begin{bmatrix} \frac{\partial L}{\partial \mathbf{x}}^T + \frac{\partial \mathbf{F}}{\partial \mathbf{x}}^T \Lambda_\mathbf{F}{}^c \\ \frac{\partial L}{\partial \mathbf{u}}^T + \frac{\partial \mathbf{F}}{\partial \mathbf{u}}^T \Lambda_\mathbf{F}{}^c \end{bmatrix}$$

Coupling Schematic

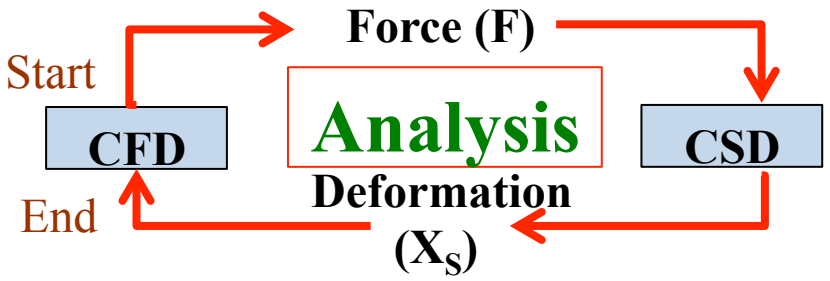

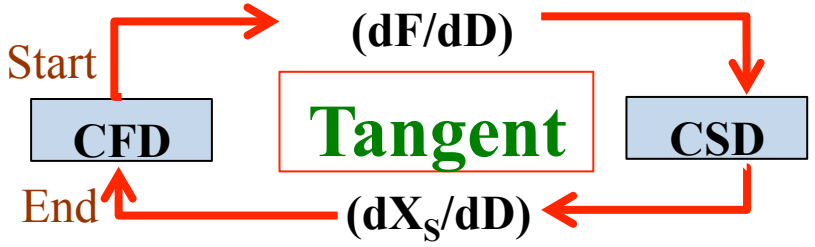

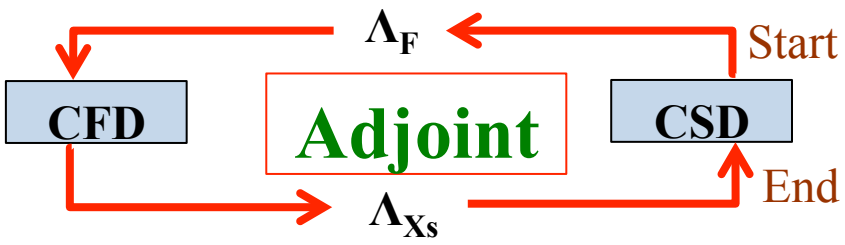

Outline

- Introduction
- Background
- Motivation & Objective
- Coupled CFD/CSD Adjoint
- Results
  - Hart-II blade optimization in hover
  - Hart-II blade optimization in Forward Flight: Thrust and moment trim, Shape Optimization and Retrim
- Conclusion

Hover (Unsteady) Test Problem

- 4 bladed Hart-II rotor in hover:
  - Rigid & Flexible; M_{tip} = 0.64; 1040 RPM
- CFD/CSD specifications:
  - 2.32 & 11.4 million grid nodes (prisms, pyramids, tets)
  - 20 beam elements
- Tight CFD/CSD coupling
  - 1 rotor revs
  - 2.32M : dt=2^{O}, 1^{O}, 0.5^{O}
    - 6 coupling per time step, **10** CFD and 20 CSD non-linear iterations per coupling
    - ~1 hr/rev with 512 cores
  - 11.4M: dt = 2^{O}
    - 6 coupling per time step, **25** CFD and 20 CSD non-linear iterations per coupling
    - ~2.5 hr/rev with 2048 cores

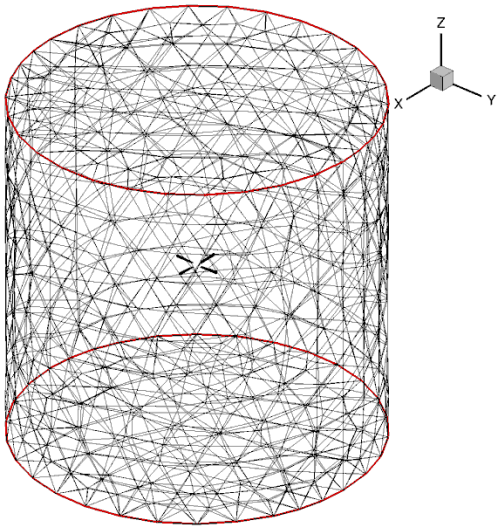

CFD flow domain

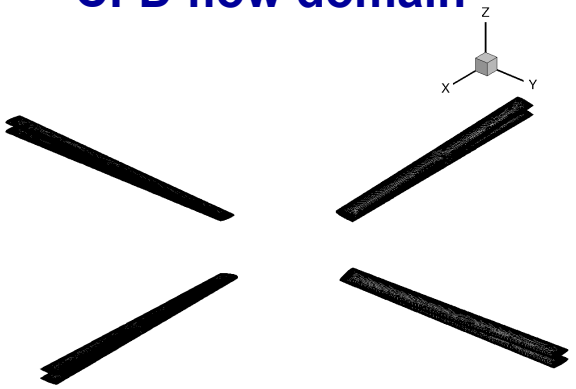

Rigid and Flexible blades

Blade Geometry Parametrization

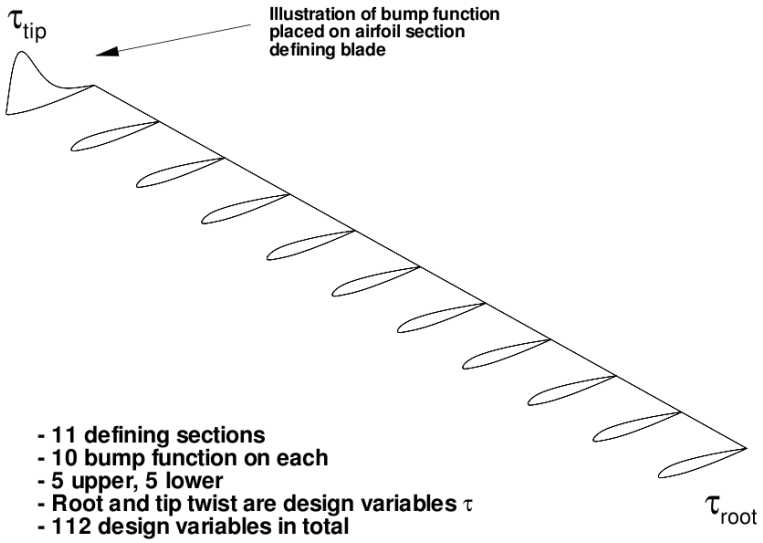

Hicks-Henne bump functions

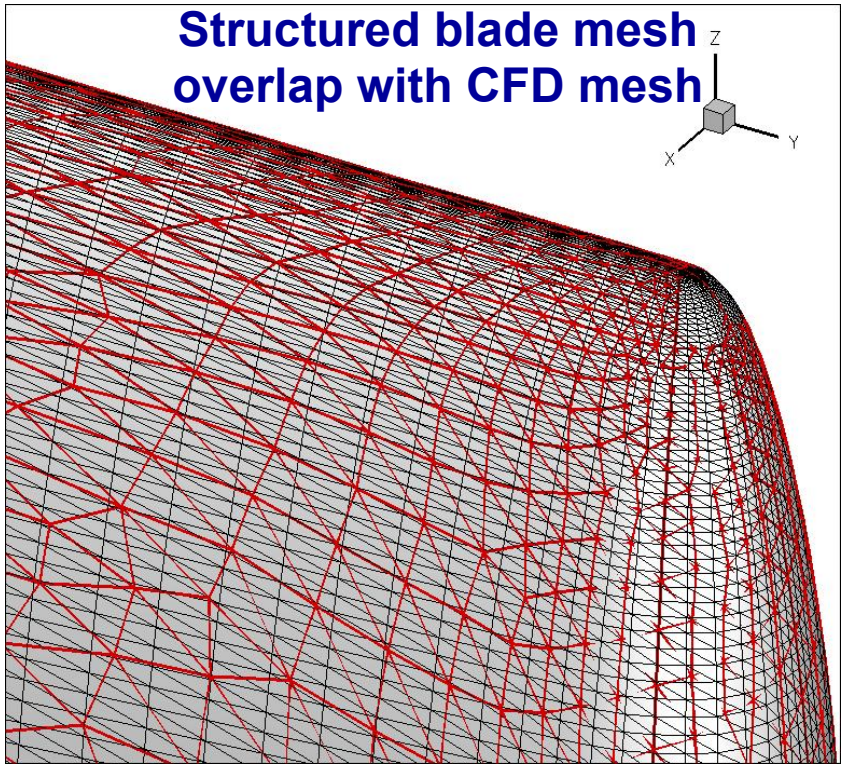

- Master blade shape defined by Hicks-Henne bump functions and twist
  - Defined by high-resolution structured mesh (in black)
  - Shape changes interpolated onto unstructured CFD surface mesh
- 112 design parameters
  - 10 Hicks-Henne bump functions per blade section, 11 blade sections (110)
  - Twist at blade root and tip (2)

Unsteady Objective Function

- Unsteady objective function:

$$L^n = (\delta C_T^n)^2 + 10(\delta C_Q^n)^2$$
$$\delta C_T^n = (C_T^n - C_{T\,target}^n)$$
$$\delta C_Q^n = (C_Q^n - C_{Q\,target}^n)$$

- Minimize torque with thrust constrained to value of the baseline Hart-II rotor
- Global functional:

$$L^g = \frac{1}{T}\sum_{n=1}^{n=N} \Delta t L^n$$

- $C_{T,target}$ from baseline Hart-II
- $C_{Q,target}$ is set to zero (to be minimized)

Unsteady Strongly Coupled CFD/CSD Adjoint Sensitivity Verification

- Tangent and adjoint verification by perturbing tip twist (i.e. **D**=tip twist)
- Complex perturbation of value $1x10^{-100}$
- $\partial L \uparrow n / \partial \boldsymbol{D}$ from **tangent** and **adjoint** verified with **complex step method** every time step
- Three sensitivity analysis formulations converged to machine zero every time step

Verification of Strongly Coupled CFD/CSD Adjoint Formulation

- Verified to 12 significant digits
- Verified over multiple time steps
- Accuracy preserved over multiple time-steps

Time step	Method	$\partial L\hat{}n / \partial D$
1	Complex	3.690007037237**534**E-006
	Tangent	3.690007037237**471**E-006
	Adjoint	3.690007037237**598**E-006
2	Complex	5.150483530831**191**E-006
	Tangent	5.150483530831**145**E-006
	Adjoint	5.150483530831**289**E-006
3	Complex	5.828069793498**591**E-006
	Tangent	5.828069793498**538**E-006
	Adjoint	5.828069793498**741**E-006
4	Complex	6.056211086344**925**E-006
	Tangent	6.056211086344**902**E-006
	Adjoint	6.056211086345**518**E-006
5	Complex	6.026286742020**757**E-006
	Tangent	6.026286742020**644**E-006
	Adjoint	6.026286742020**636**E-006

Strongly Coupled Optimization on Hart-II Rotor: 2.32M Grid

- Optimization over 1 rev: dt=2.0^o ,1.0^o , 0.5^o
- Optimizer: L-BFGS-B bounded reduced Hessian
- Bounds:
  - $\pm 5\%$ chord on airfoil section
  - $\pm 1.0^o$ twist
- 6 coupling cycles/time-step, 10 Newton cycles/coupling
- Parallel with 512 cores

Optimized vs Baseline Performance (dt=2 deg)

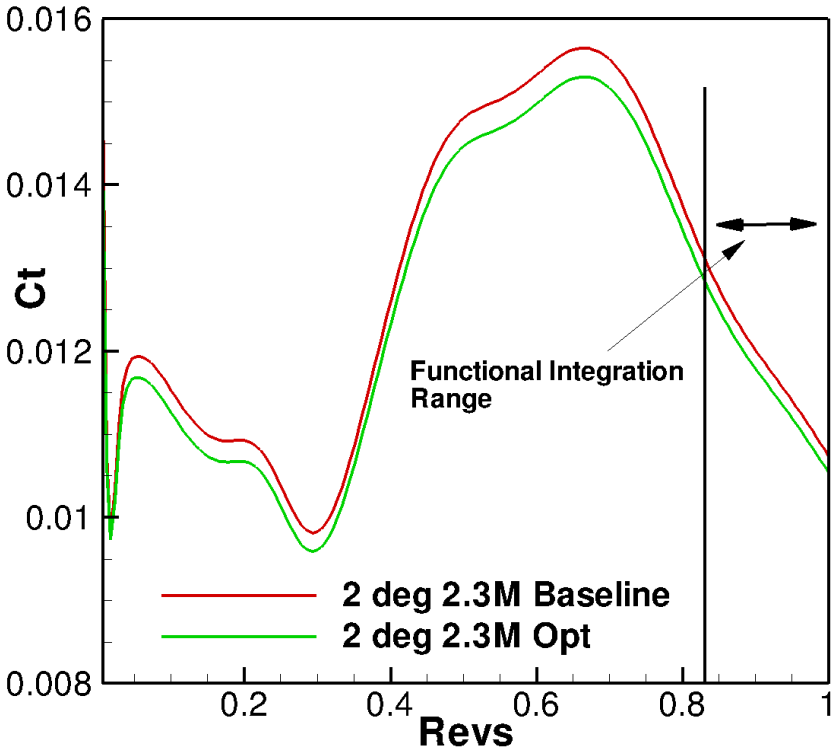

Thrust vs time

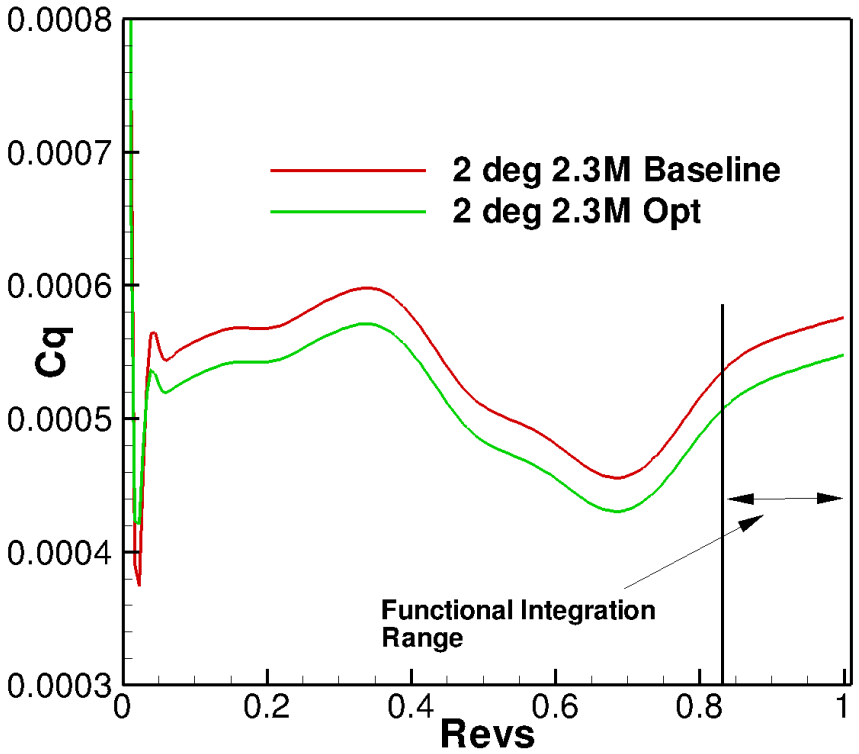

Power vs time

- 4.9% power reduction with 1.8% thrust loss penalty

Optimized vs Baseline Performance (dt=1 deg)

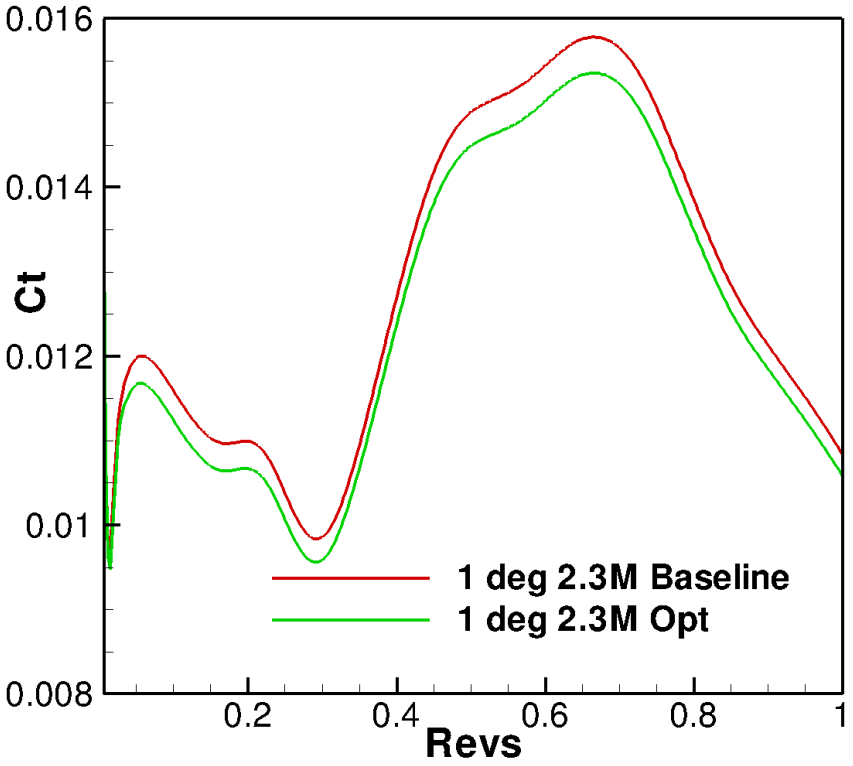

Thrust vs time

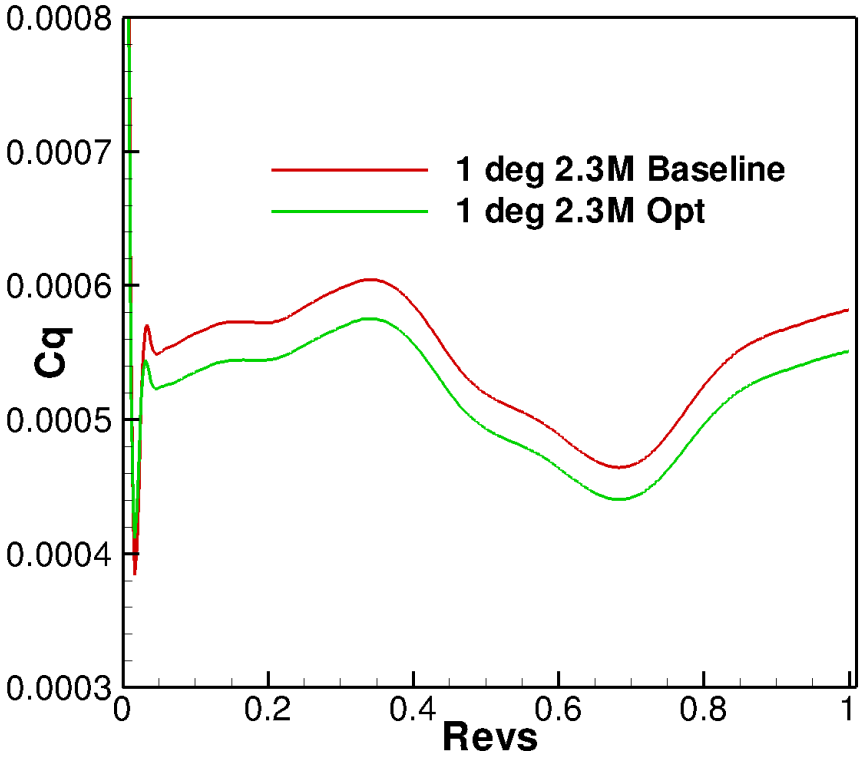

Power vs time

- 5.3% power reduction with less than 2.3% thrust reduction

Optimized vs Baseline Performance (dt=0.5 deg)

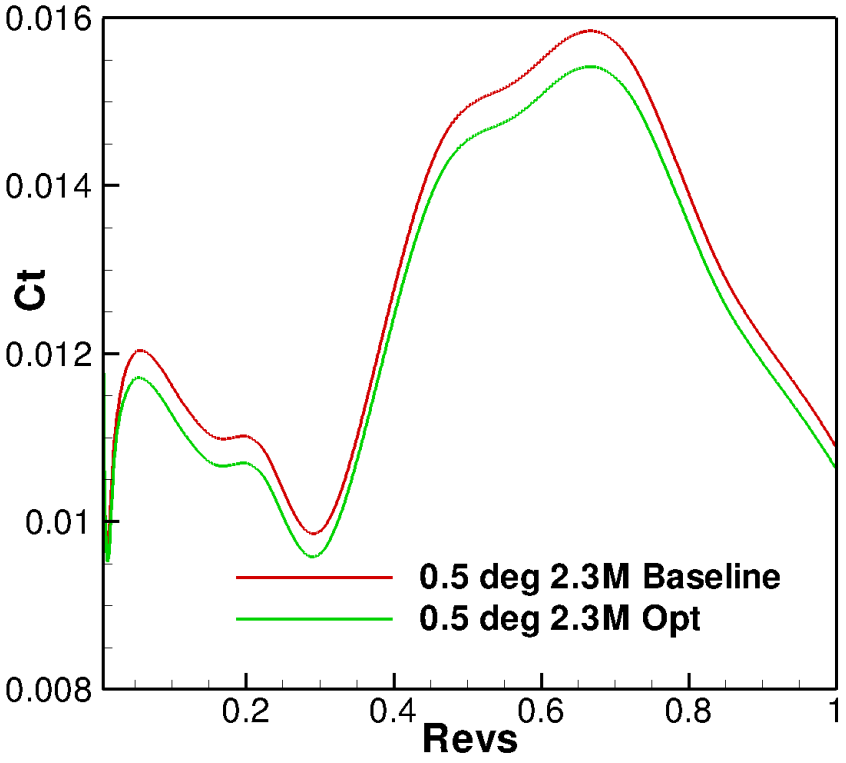

Thrust vs time

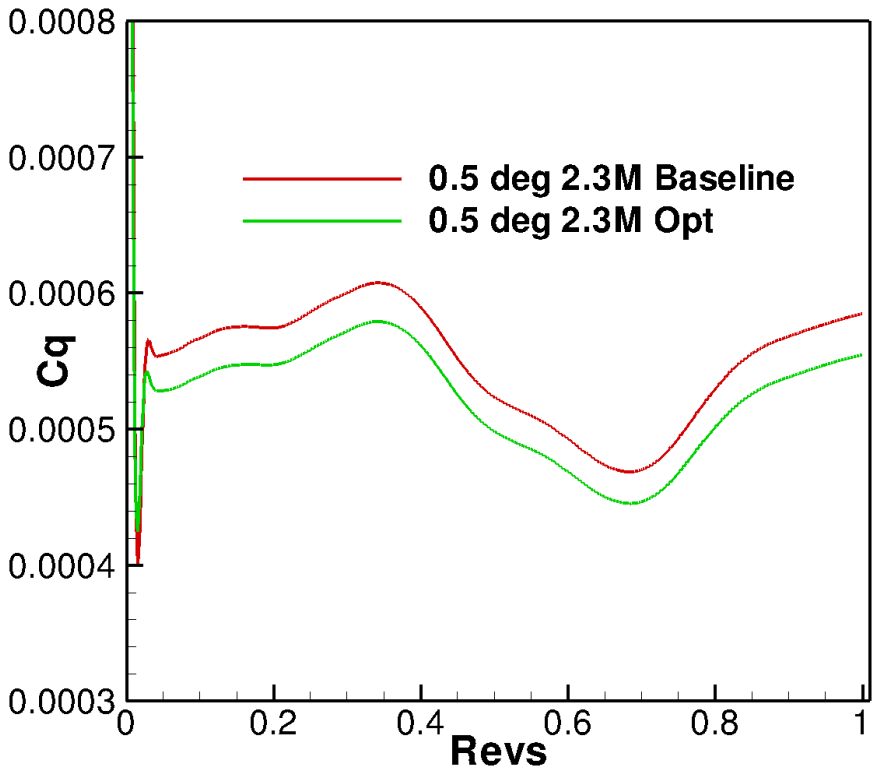

Power vs time

- 5.2% power reduction with less than 2.4% thrust reduction

Blade Optimization Results

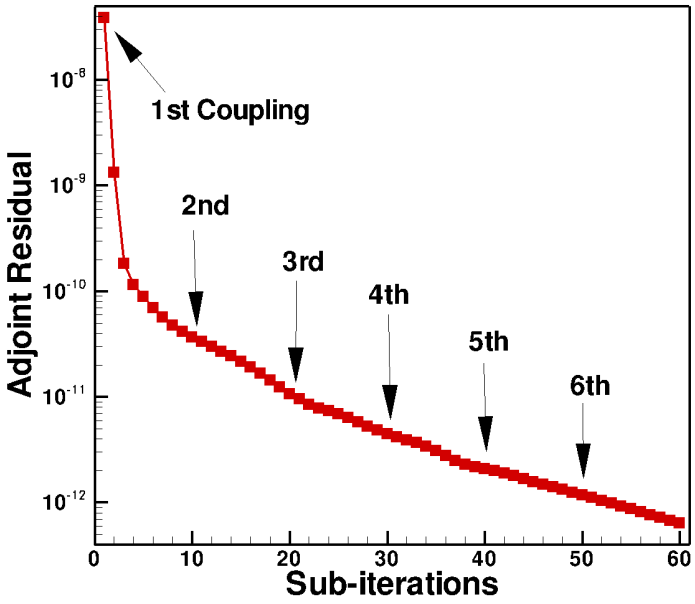

Adjoint flow residual

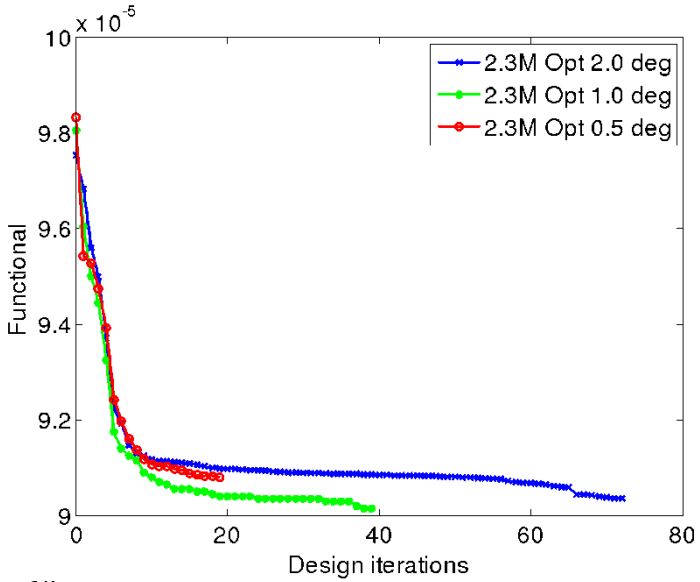

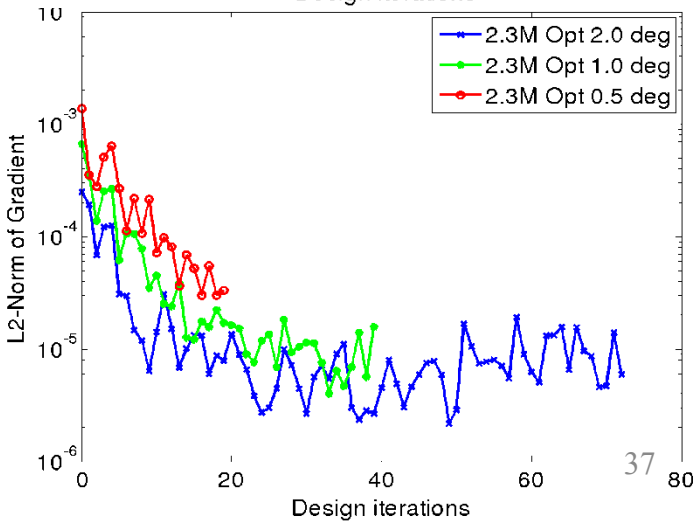

- Adjoint flow residual convergence by 5 orders
- Functional plateaus, gradient drops by 2 orders

Optimized Blade Sections

Baseline

Opt 2.0 deg

Opt 1.0 deg

Opt 0.5 deg

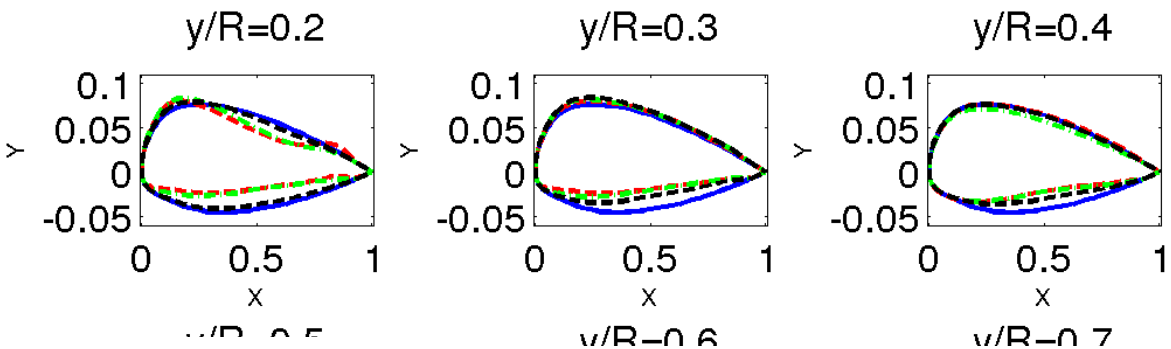

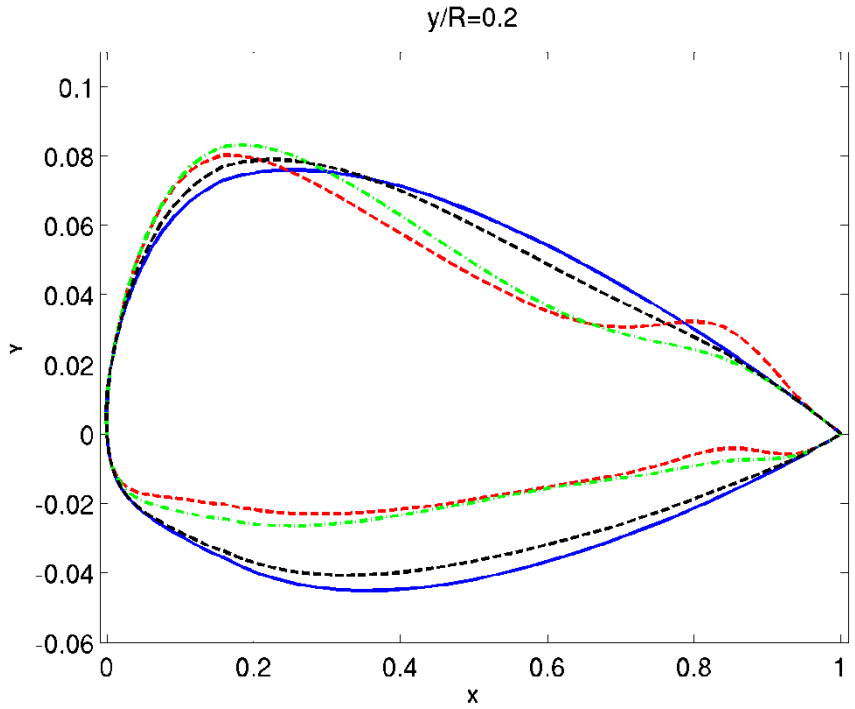

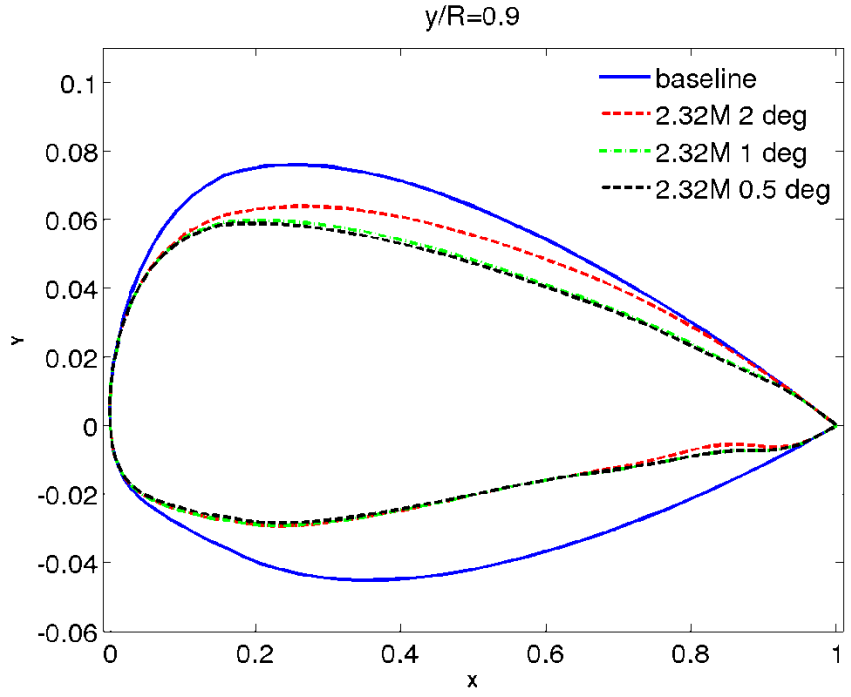

Optimized vs Baseline Performance (10 revs, dt=2 deg)

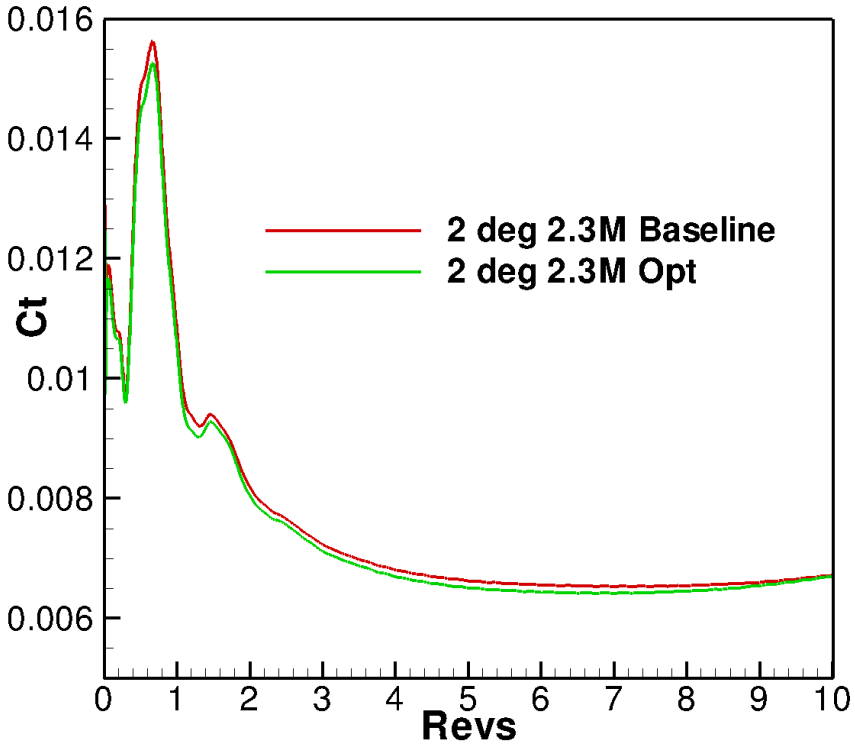

Thrust vs time

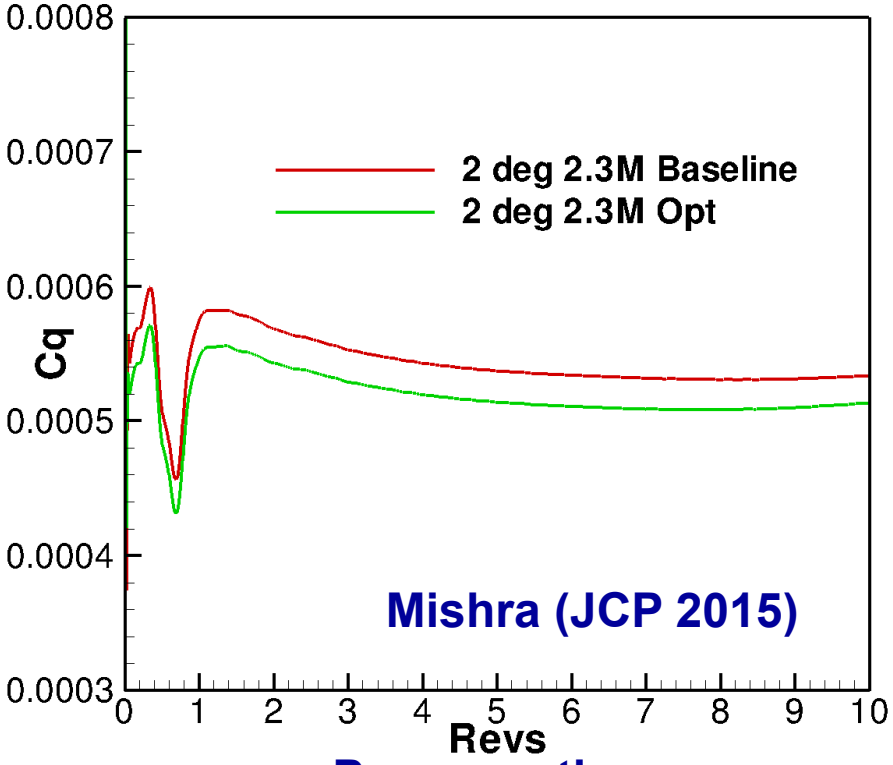

Power vs time

- 5% power reduction with less than 2% thrust penalty

Outline

- Introduction
- Background
- Motivation & Objective
- Coupled CFD/CSD Adjoint
- Results
  - Hart-II blade optimization in hover
  - Hart-II blade optimization in Forward Flight: Thrust and moment trim, Shape Optimization and Retrim
- Conclusion

Forward Flight (Unsteady) Test Problem

- 4 bladed Hart-II rotor in forward flight:
  - Rigid & Flexible; M_{tip} = 0.64; 1040 RPM; μ=0.15 (Minf~0.1); $\alpha=5.4^{O}$
- CFD/CSD specifications:
  - 2.32 million grid nodes (prisms, pyramids, tets)
  - 20 beam elements per blade
- Tight CFD/CSD coupling
  - 2 rotor revs
  - 2.32M : $\Delta t=2^{O}$
    - 6 coupling per time step, **10** CFD and 20 CSD non-linear iterations per coupling
    - ~40 min/rev with 1024 cores
  - Control Inputs:
    - Collective (θ_O)and Cyclics (θ_{1c}, θ_{1s})

$$\theta_{pitch} = \theta_O + \theta_{1c}\cos\psi + \theta_{1s}\sin\psi$$

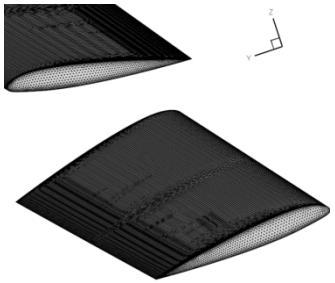

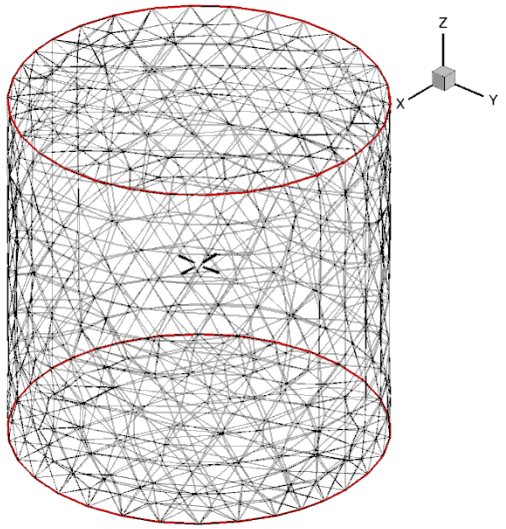

CFD flow domain

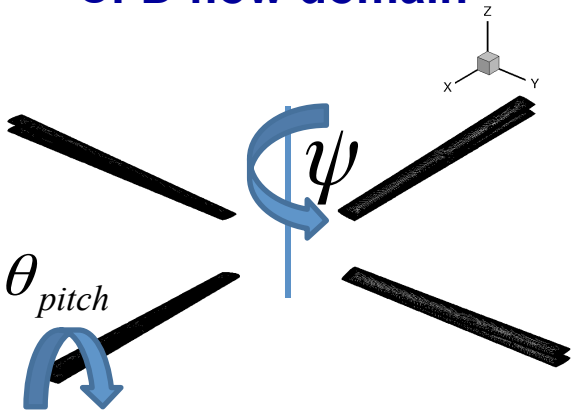

Rigid and Flexible blades

Blade Geometry Parametrization

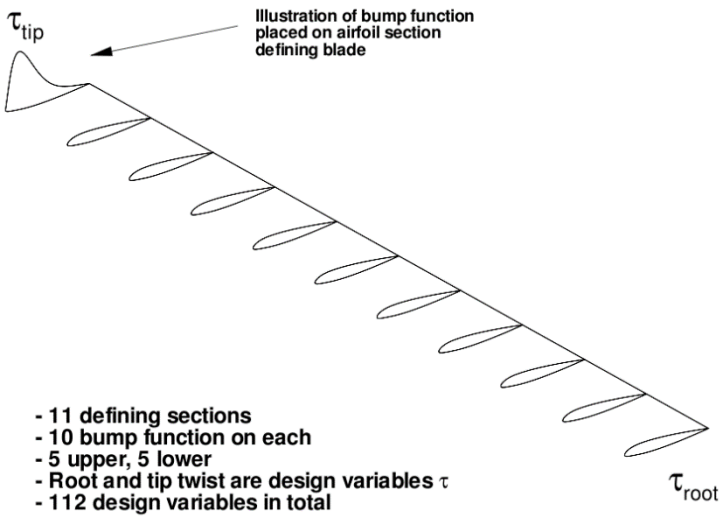

Hicks-Henne bump functions

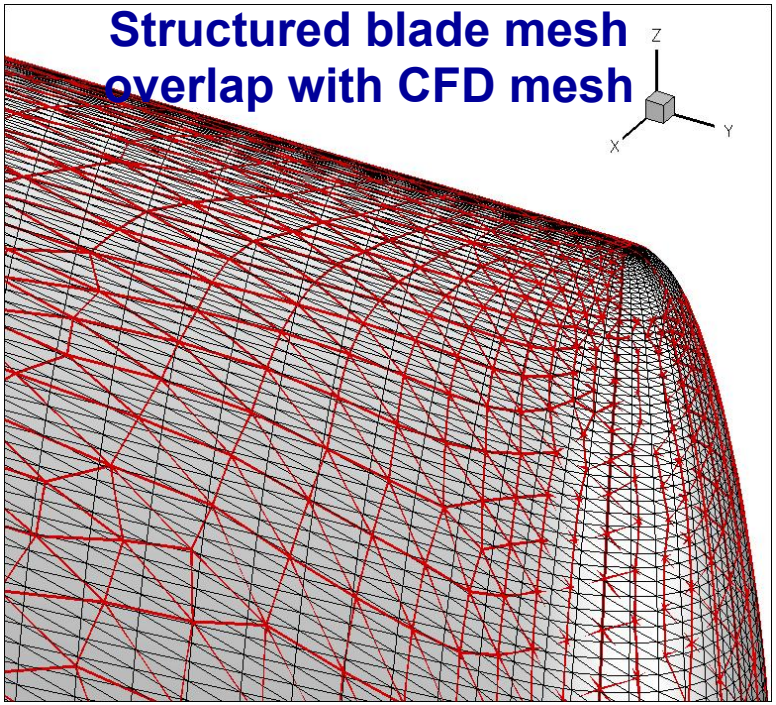

- Master blade shape defined by Hicks-Henne bump functions and twist
  - Defined by high-resolution structured mesh (in black)
  - Shape changes interpolated onto unstructured CFD surface mesh
- 115 design parameters
  - 10 Hicks-Henne bump functions per blade section, 11 blade sections (110)
  - Twist at blade root and tip (2) and 3 pitch parameters $\theta_{pitch} = \theta_O + \theta_{1c}\cos\psi + \theta_{1s}\sin\psi$

Unsteady Objective Function

$$\min L = L_{power} + \omega L_{trim}$$

$$L_{power} = \frac{1}{T}\sum_{n=1}^{n=N} \Delta t\left[\delta C_Q^n\right]^2$$

$$L_{trim} = \omega_1 \frac{1}{T}\sum_{n=1}^{n=N} \Delta t\left[\delta C_T^n\right]^2 + \omega_2\left[\delta \overline{C}_{Mx}\right]^2 + \omega_3\left[\delta \overline{C}_{My}\right]$$

$$\delta C_Q^n = (C_Q^n - C_{Q_{TARGET}}^n)$$

$$\delta C_T^n = (C_T^n - \overline{C}_{T_{TARGET}}^n)$$

$$\delta \overline{C}_{My} = \frac{1}{T}\sum_{n=1}^{n=N} \Delta t(C_{My}^n - C_{My_{TARGET}}^n)$$

$$\delta \overline{C}_{Mx} = \frac{1}{T}\sum_{n=1}^{n=N} \Delta t(C_{Mx}^n - C_{Mx_{TARGET}}^n)$$

- Trim

  Target thrust = 4.4e-3

  Target C_{Mx} C_{My}=0.0

- Performance
  - Target power = 0.0

Unsteady Strongly Coupled CFD/CSD Adjoint Sensitivity Verification

- Tangent and adjoint verification by perturbing collective pitch (i.e. $\mathbf{D}=\theta_O$)
- Complex perturbation of value $1x10^{-100}$
- $\partial L\hat{\uparrow}n / \partial \boldsymbol{D}$ from **tangent** and **adjoint** verified with **complex step method** every time step
- Three sensitivity analysis formulations converged to machine zero every time step

Verification of Strongly Coupled CFD/CSD Adjoint Formulation

- Verified to 10 significant digits
- Verified over multiple time steps
- Accuracy preserved over multiple time-steps

Mishra (AIAAJ 2016)

Time step	Method	$\partial L\hat{}n / \partial D$
1	Complex	7.569817143673123E-005
	Tangent	7.569817143673061E-005
	Adjoint	7.569817143672761E-005
2	Complex	6.040142779349352E-005
	Tangent	6.040142779349835E-005
	Adjoint	6.040142779349570E-005
3	Complex	-4.959909870786381E-006
	Tangent	-4.959909870787765E-006
	Adjoint	-4.959909870785228E-006
5	Complex	-1.142069116982308E-004
	Tangent	-1.142069116982308E-004
	Adjoint	-1.142069116982432E-004
180	Complex	-5.176189427439016E-003
	Tangent	-5.176189427439005E-003
	Adjoint	-5.176189427434507E-003

Optimization Procedure

1:Trim rotor
- Minimize L_{trim} (drive to 0)
- Using only control inputs as design parameters

2: Perform optimization
- Minimize $L_{design}=L_{performance} + L_{trim}$
- Using shape parameters + control inputs (design)

3: Retrim shape-optimized rotor
- $L_{trim}=0$ not maintained exactly in design process (implemented as penalty term)

- First perform for rigid rotor, then flexible rotor

Strongly Coupled Optimization on Hart-II Rotor: 2.32M Grid

- Optimization (trim/shape) over 2 rev: $\Delta t = 2.0^o$
- Optimizer: L-BFGS-B bounded reduced Hessian
- Bounds for shape parameters:
  - $\pm 5\%$ chord on airfoil section
  - $\pm 1.0^o$ twist
- Bounds for control inputs
  - θ_o, θ_{1c}, θ_{1s} : $\pm 5.0^o$
- 6 CFD-CSD coupling cycles/time-step, 10 Newton cycles/coupling
- Run in parallel using 1024 cores
  - 70 minutes per rotor revolution (forward+adjoint)

Rigid Hart-II Forward Flight Trim

Mishra (AIAAJ 2016)

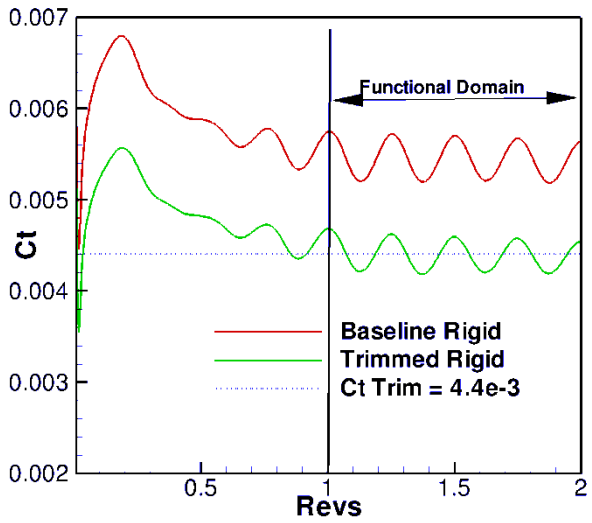

Thrust vs time

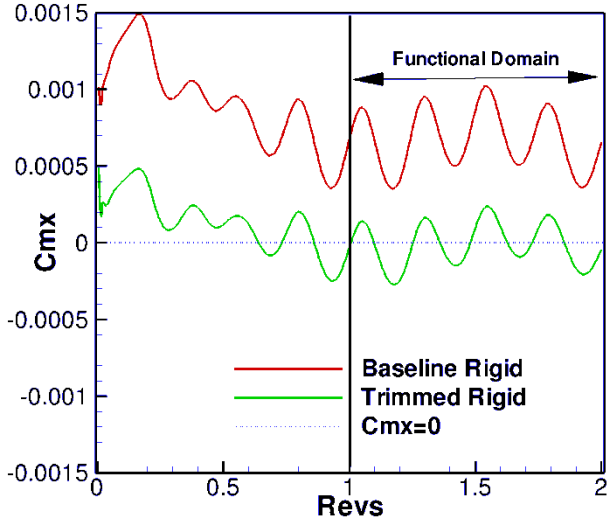

Lateral Moment vs time

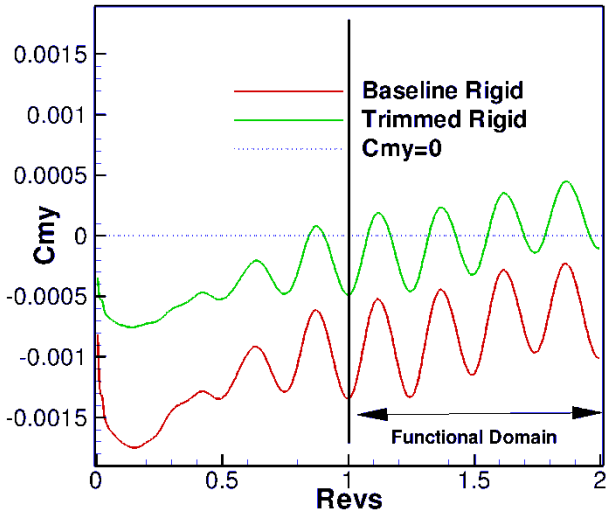

Long. Moment vs time

- Trimmed to target mean thrust (Ct=4.4e-3), zero moments (~1e-5)

Pitch (deg)	Experiment	HOST	Present (Rigid)
θ_O (Collective)	3.20	4.91	4.22
θ_{1c} (Lat. Cyclic)	2.00	1.41	0.90
θ_{1s} (Long. Cyclic)	-1.10	-1.34	-1.77

Rigid Rotor Trim Convergence

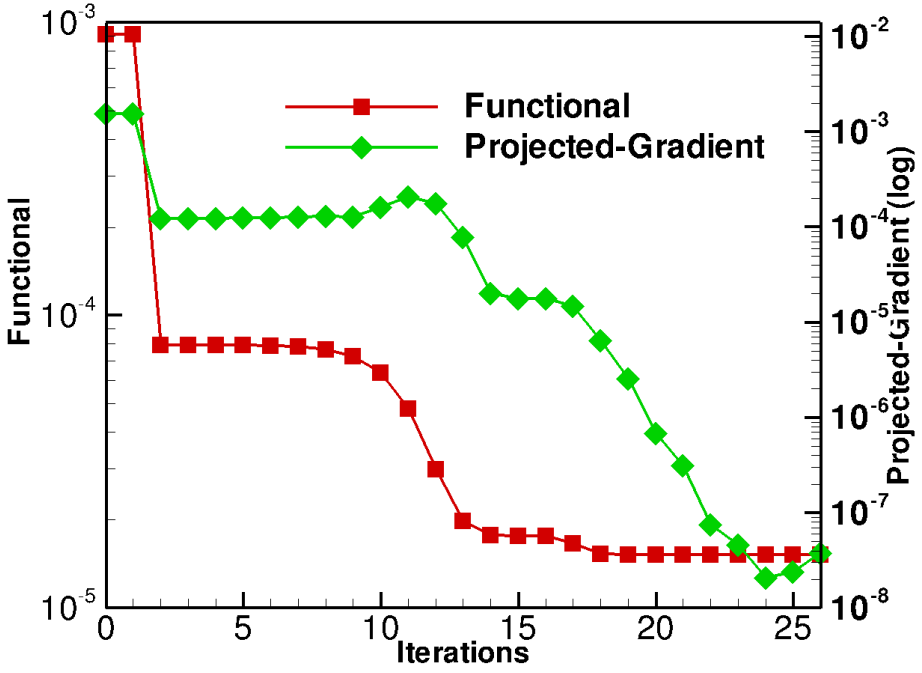

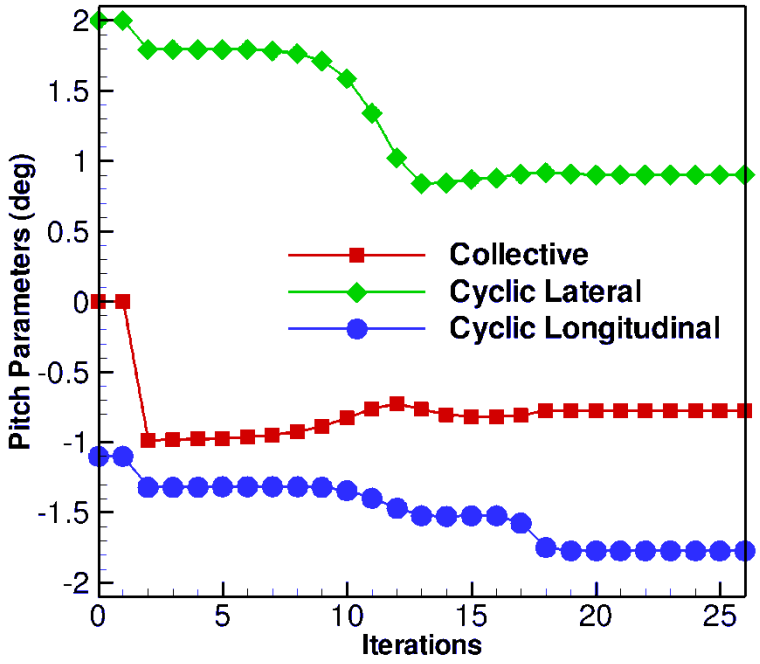

- Gradient drops more than 5 orders
- Objective converges by ~15 iterations
- Pitch parameters show consistent convergence

Rigid Hart-II Shape Optimization

Power vs time

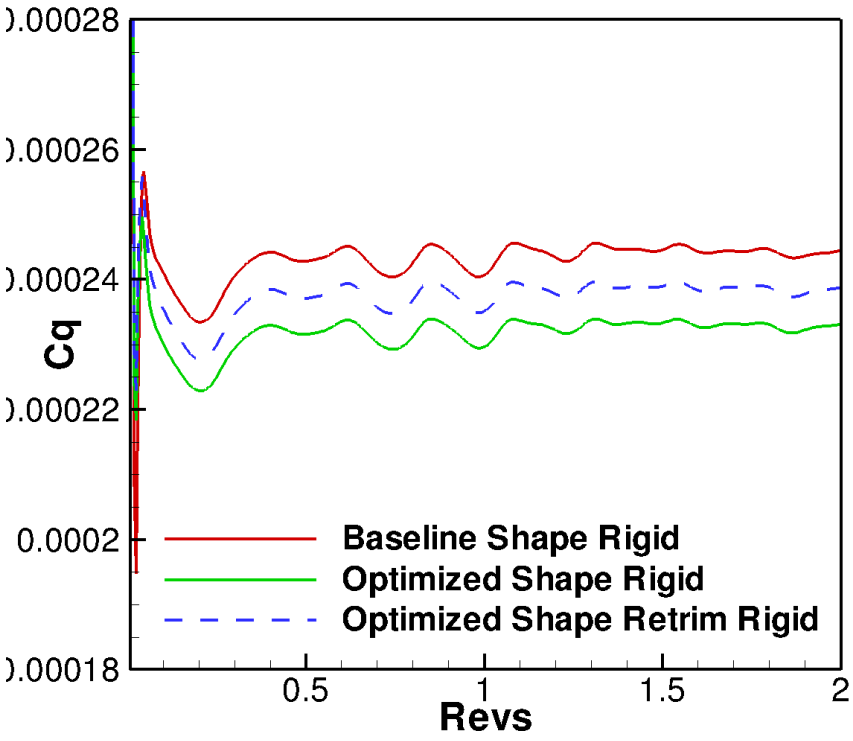

Thrust vs time

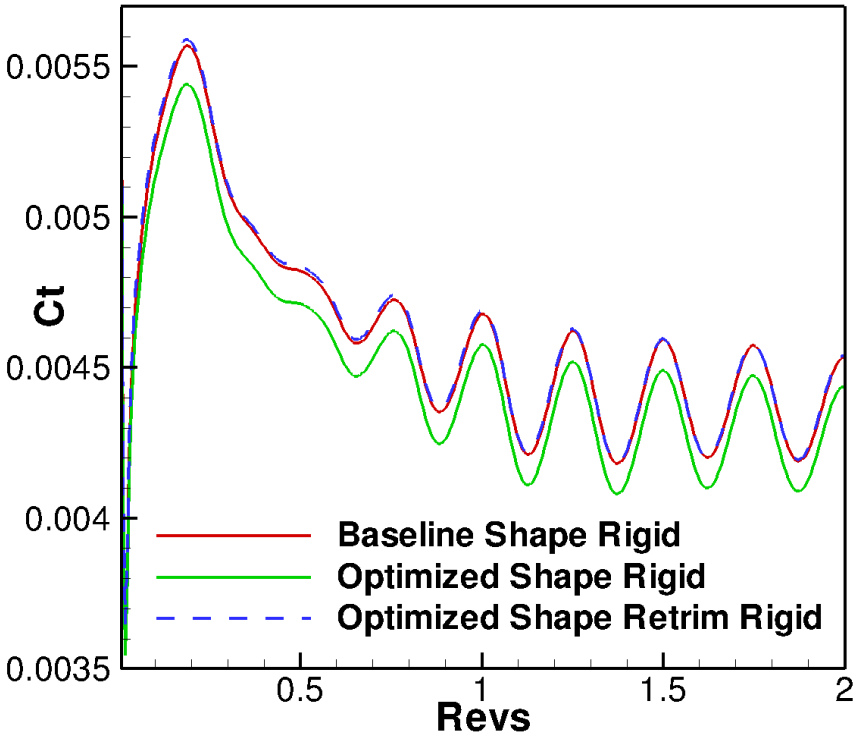

- Trimmed to target mean thrust (Ct=4.4e-3), zero moments (~1e-5)
- Overall ~**2.8**% power reduction w/ shape optimization after retrim

Mishra (AIAAJ 2016)

Rigid Optimized Blade Shape

Baseline

Optimized

Thicker inboard
and thinner
outboard sections

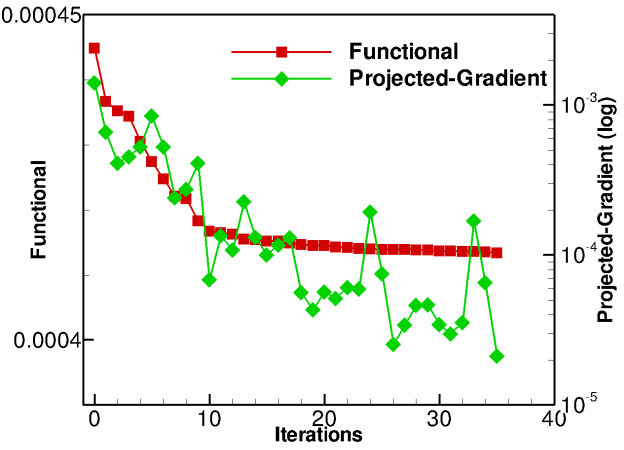

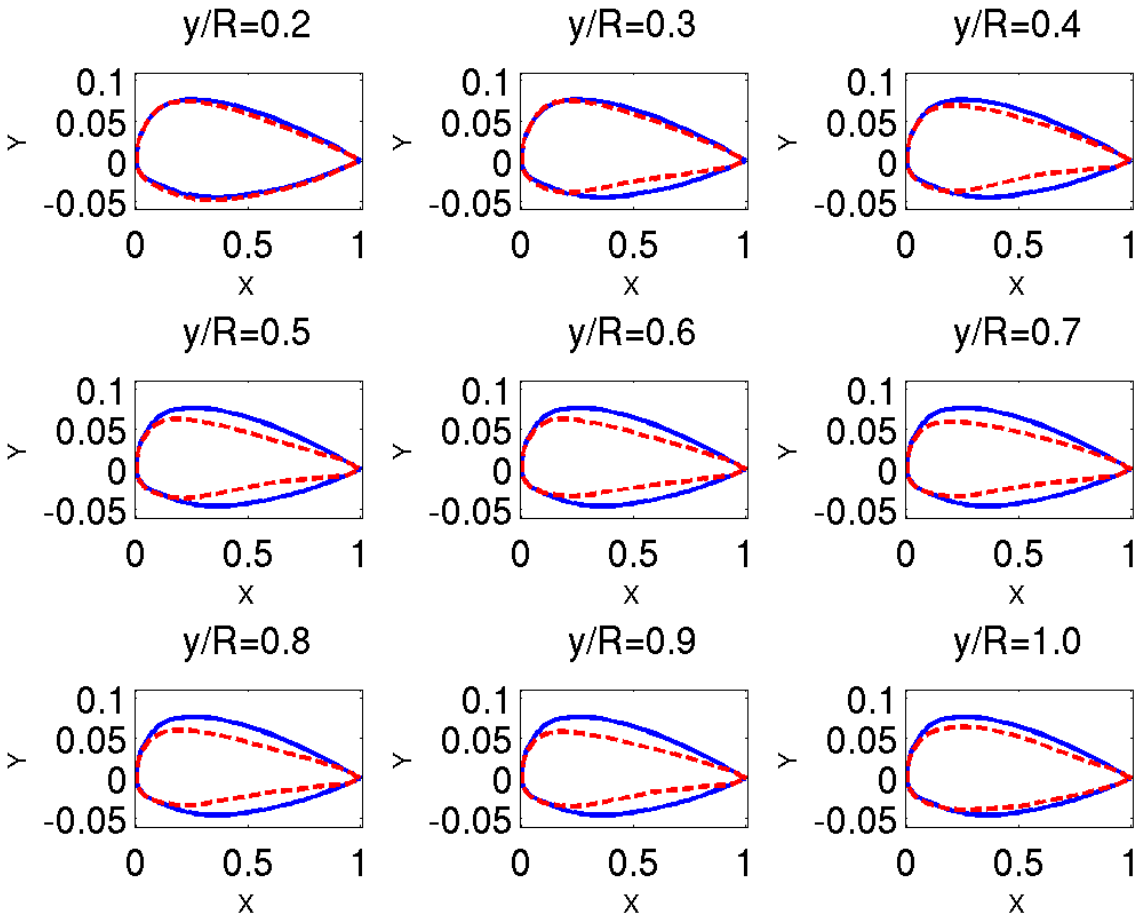

- 2 orders gradient drop, objective plateaus

Flexible Hart-II Forward Flight Trim

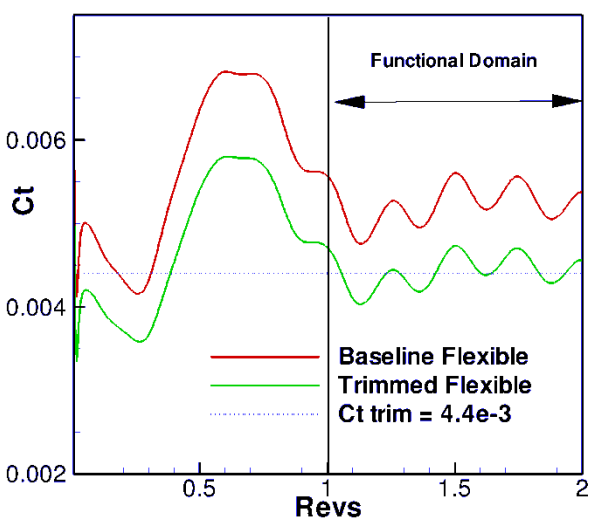

Thrust vs time

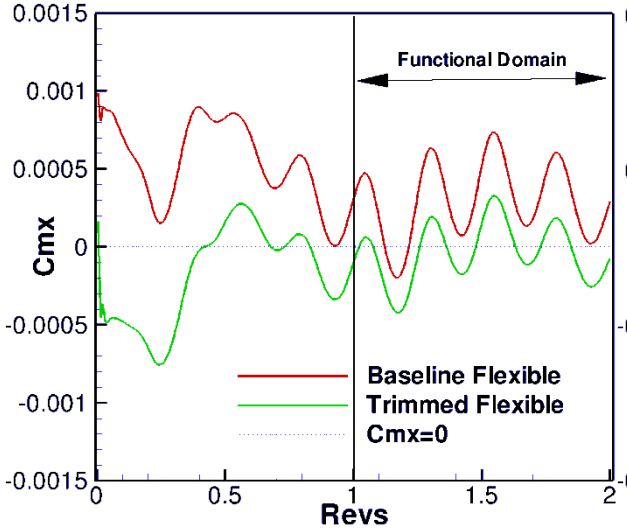

Lateral Moment vs time

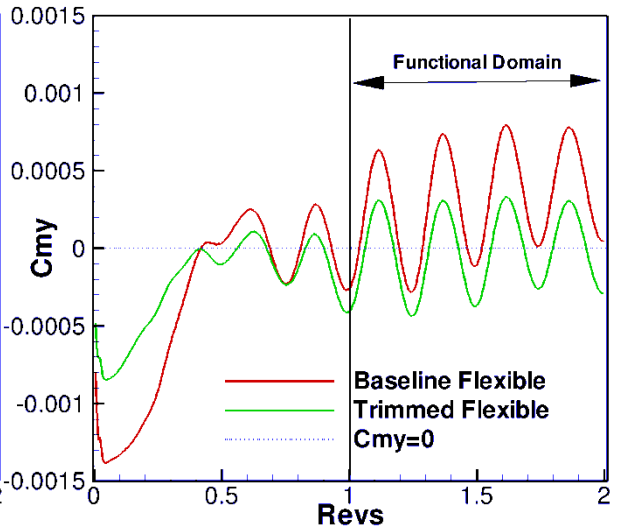

Long. Moment vs time

- Trimmed to target mean thrust (Ct=4.4e-3), zero moments (~1e-5)

Pitch (deg)	Experiment	HOST	Present (Flexible)
θ_O (Collective)	3.20	4.91	4.56
θ_{1c} (Lat. Cyclic)	2.00	1.41	1.28
θ_{1s} (Long. Cyclic)	-1.10	-1.34	-2.72

Flexible Rotor Trim Convergence

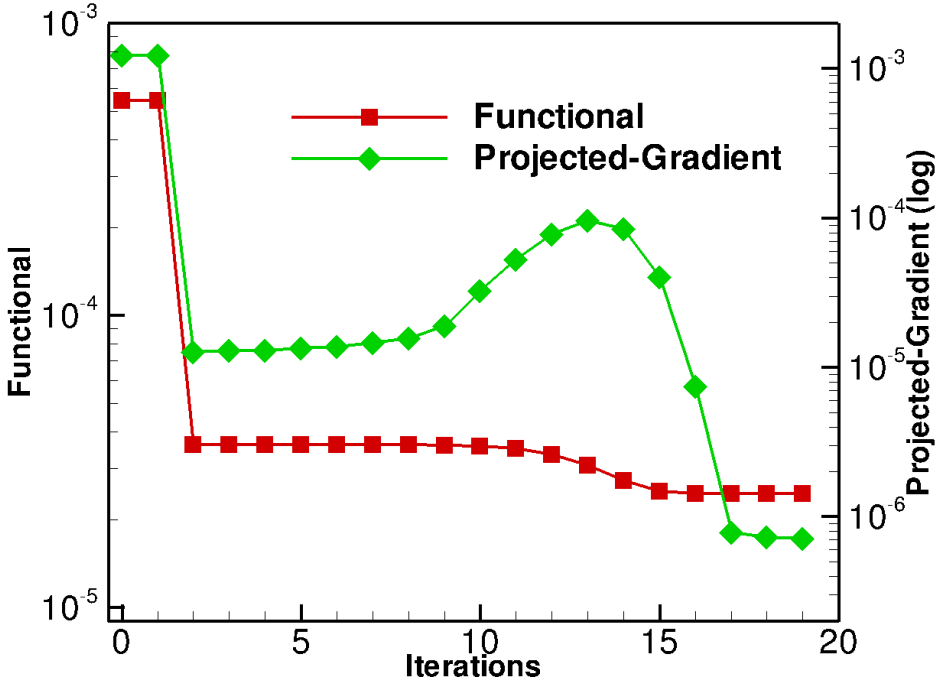

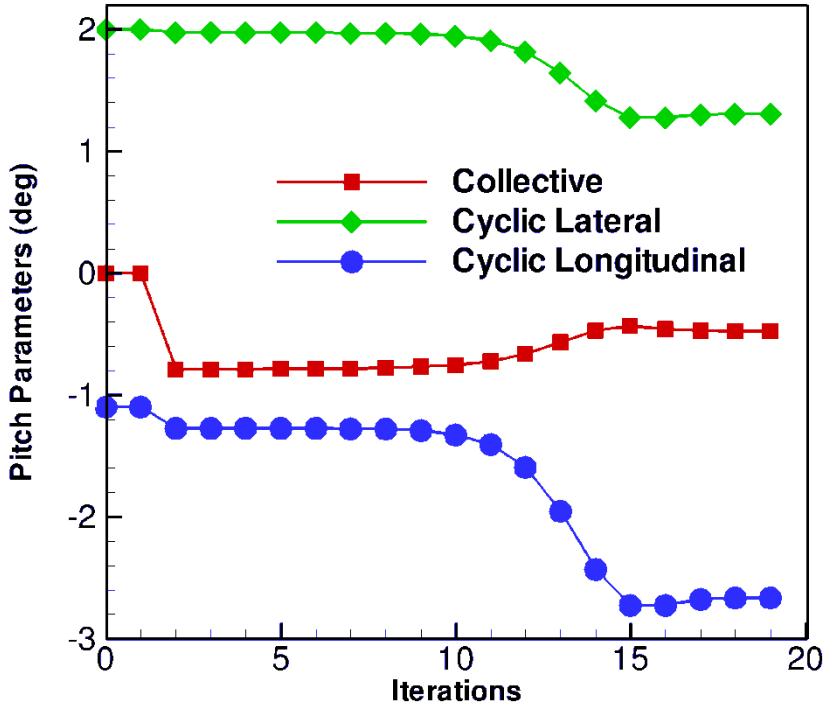

- Gradient drops more than 2 orders
- Objective converges by ~15 iterations
- Consistent pitch parameter convergence

Flexible Hart-II Shape Optimization

Power vs time

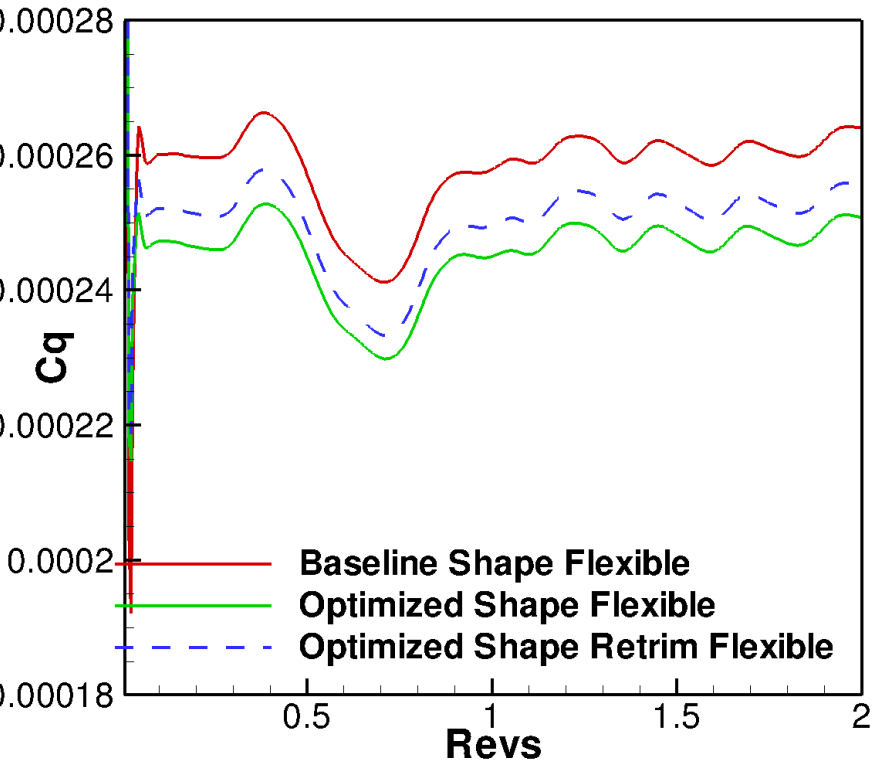

Thrust vs time

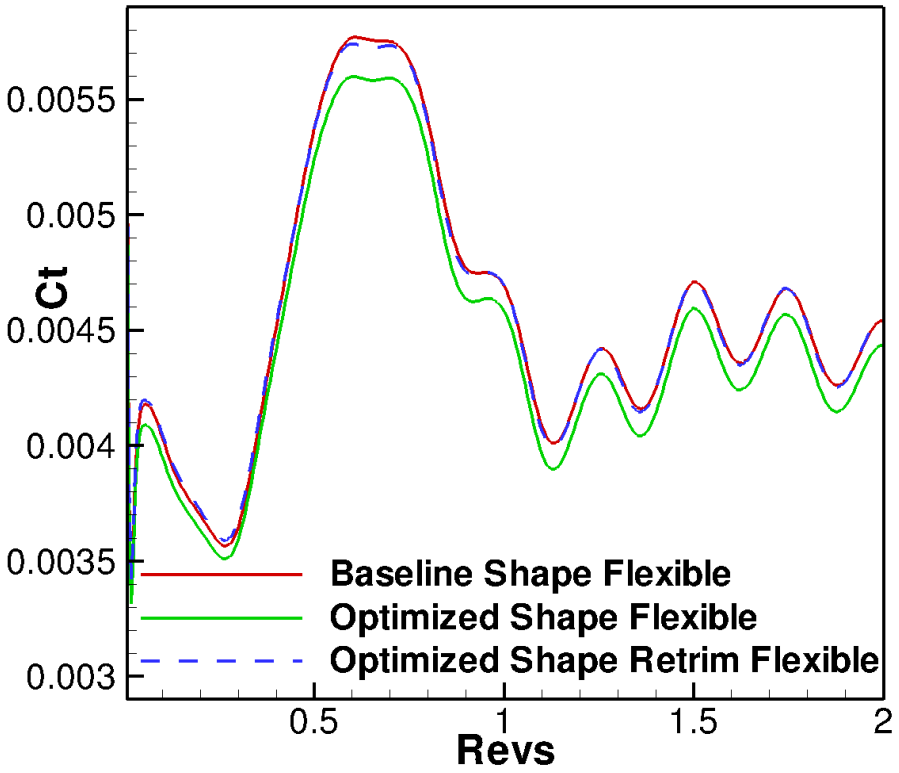

- Trimmed to target mean thrust (Ct=4.4e-3), zero moments (~1e-5)
- Overall **~3.1**% power reduction w/ shape optimization after retrim

Mishra (AIAAJ 2016)

Flexible Optimized Blade Shape

Baseline

Optimized

Thicker inboard
and thinner
outboard sections

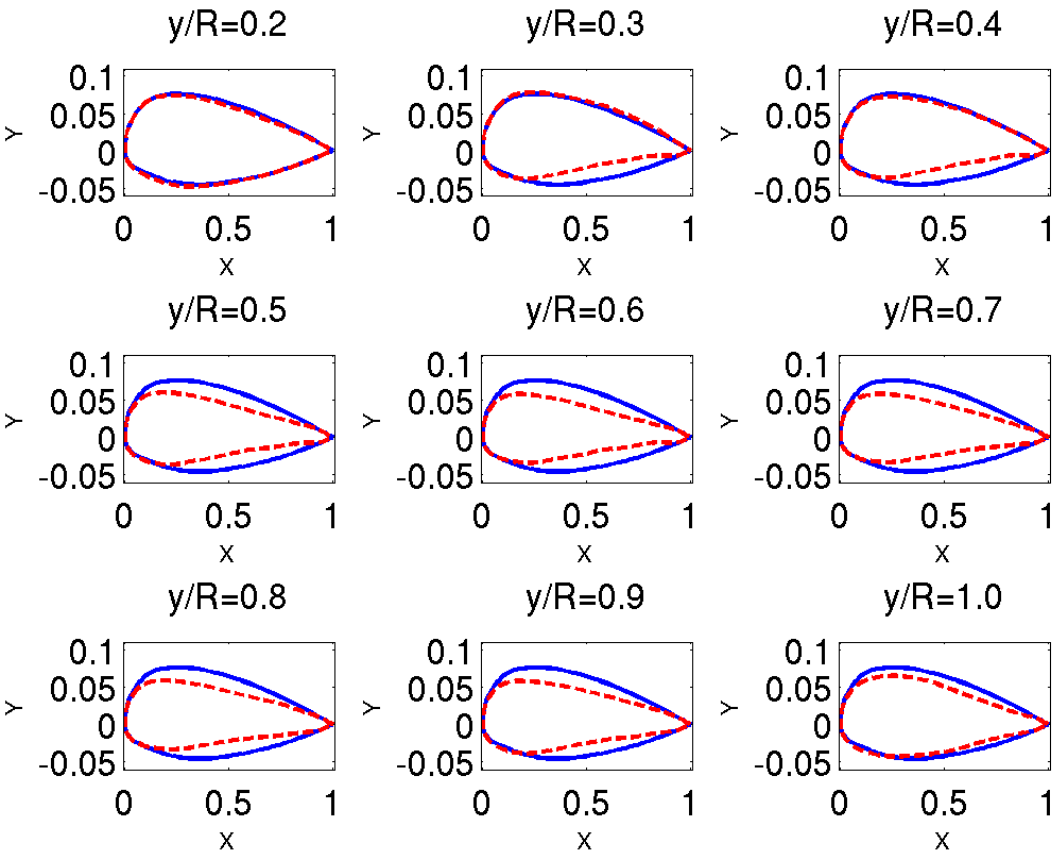

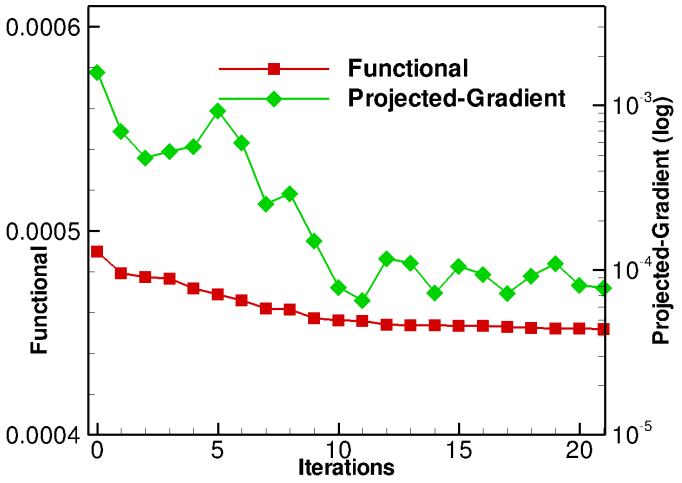

- 1 and ½ order gradient drop, objective plateaus

Multipoint Rotor Optimization

- Optimize rotor for both hover and forward flight
- At each design cycle:
  - Compute rotor performance in hover
  - Compute rotor performance in forward flight
  - Compute rotor sensitivities in hover
  - Compute rotor sensitivities in forward flight
  - Build composite performance objective function
  - Build composite objective sensitivities
  - Perform optimization step
  - Repeat

Multi-point Unsteady Objective Function

$$\min L_{MP} = \omega_{HOVER} L_{HOVER} + \omega_{CRUISE} L_{CRUISE}$$

- Weights
  - ω are weights chosen empirically to weight different operational points
  - Tests performed using:
  - $\omega_{hover} = 0.5 \quad \omega_{cruise} = 0.5$
  - $\omega_{hover} = 0.25 \quad \omega_{cruise} = 0.75$

Multi-point Design Parameters

- Hover
  - Initial: 5 deg precollective, zero cyclics
  - 1 control (collective) and 112 shape and design parameters (total=113)
- Cruise
  - Initial: Collective, $\theta_O = 4.23^O$ and Cyclics, $\theta_{1c} = 0.9^O$, $\theta_{1s} = -1.77^O$
  - 3 control (pitch) and 112 shape and design parameters (total 115)
- Total 116 design parameters
  - **Two distinct collective parameters:** $\theta_{O\_hover} \neq \theta_{O\_cruise}$

Multipoint Implementation

- Multiple design points run in parallel
- Driver routine runs on 2048 processors
  - Spawns 2 instances of solver each running on 1024
  - Each run requires 95 minutes on 1024 processors
- Parallel multipoint design cycle requires 100 minutes on 2048 processors
  - Hover analysis and adjoint
  - Cruise analysis and adjoint
  - Multipoint objective/sensitivity construction
  - Design step (shape deformation)

Rigid Multipoint Shape Optimization (ω_{hover} ,ω_{cruise}) = (0.5,0.5)

Power vs time

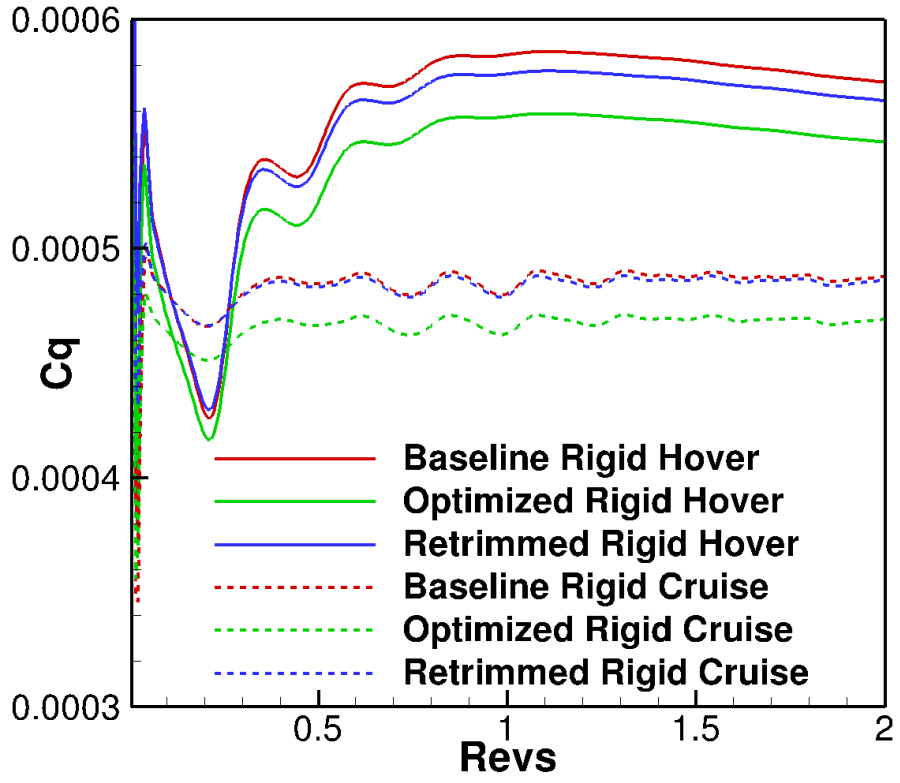

Thrust vs time

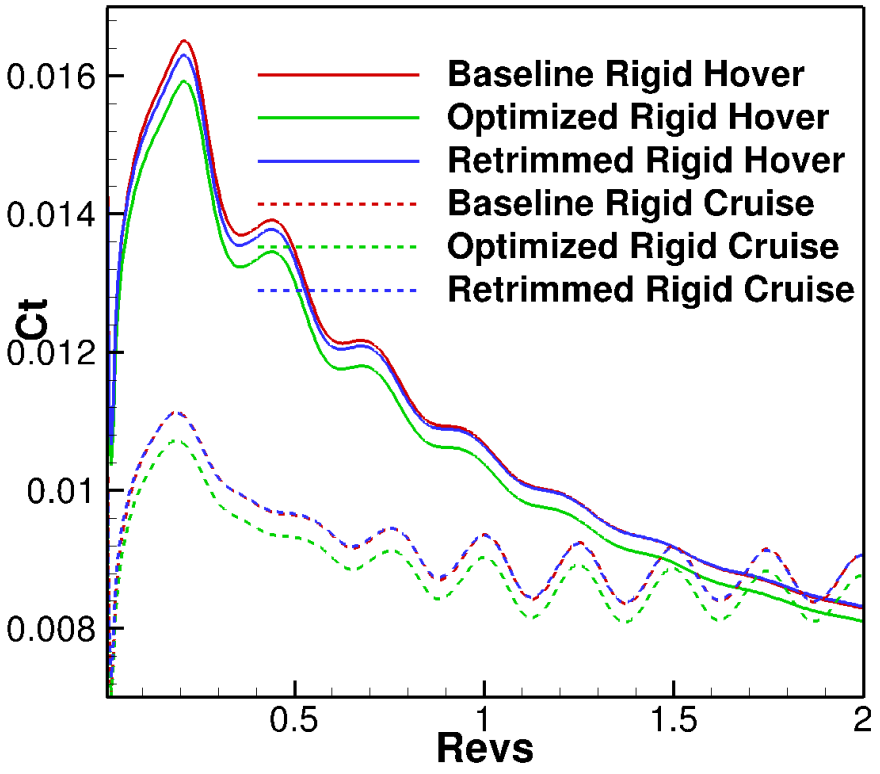

- Trimmed to target time-dependent thrust, zero moments (~1e-5)
- Overall power reduction w/ shape optimization after retrim: **~1.43**% (hover) and **~0.38**% (cruise)

Mishra (AHS 2015)

Rigid Multipoint Optimized Blade Shape (ω_{hover} ,ω_{cruise}) = (0.5,0.5)

Baseline

Optimized

Thicker inboard and thinner outboard sections

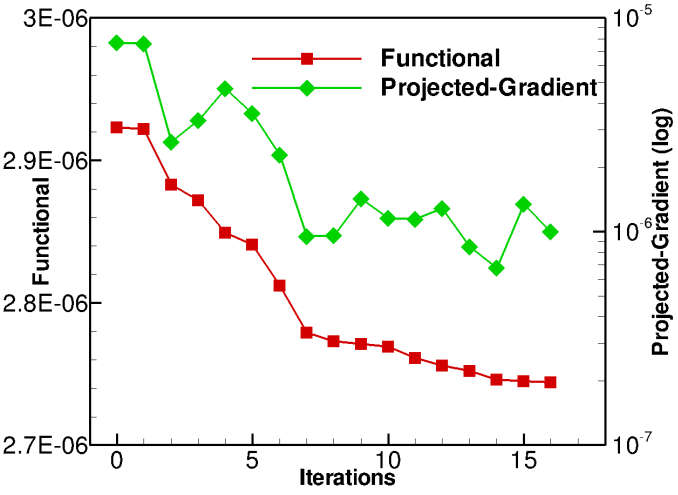

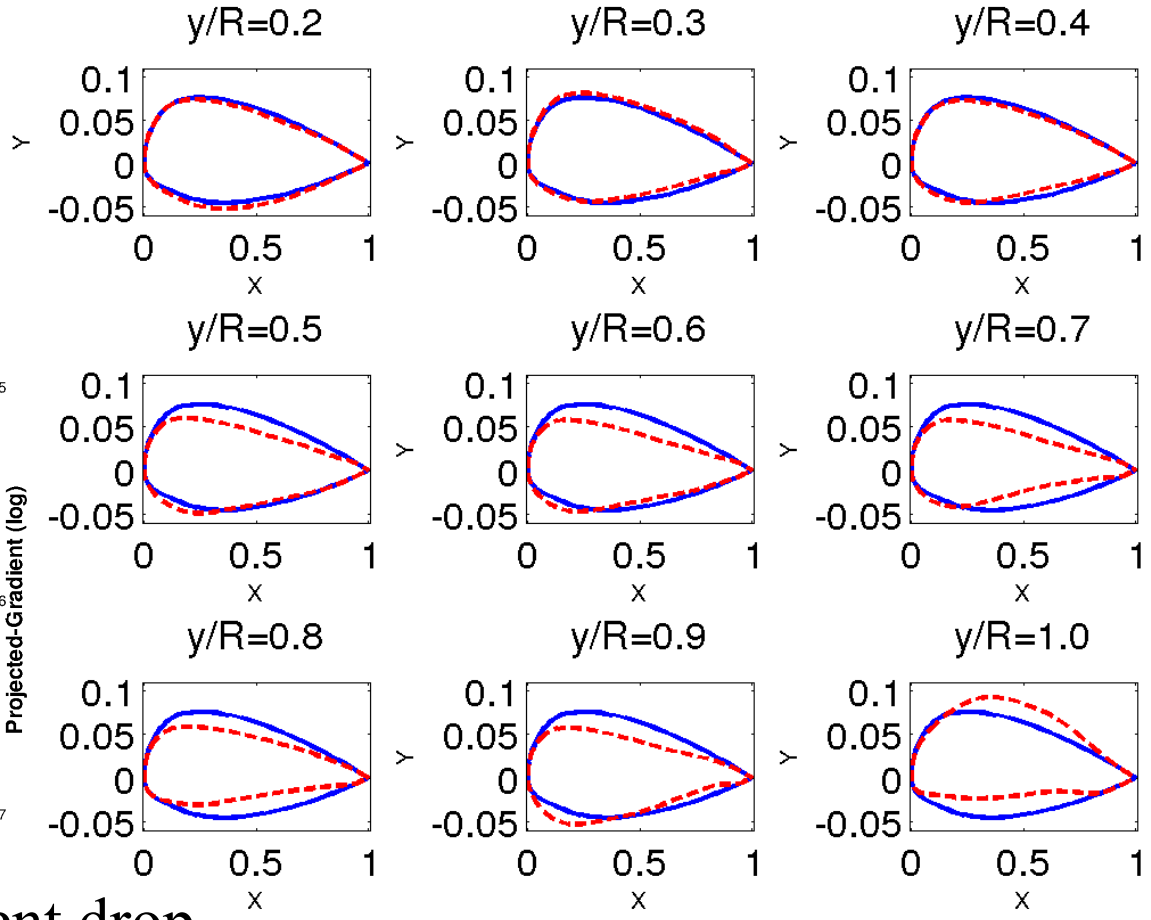

- 1 and ½ order gradient drop, objective converges

Rigid Multipoint Shape Optimization (ω_{hover} , ω_{cruise}) = (0.25,0.75)

Power vs time

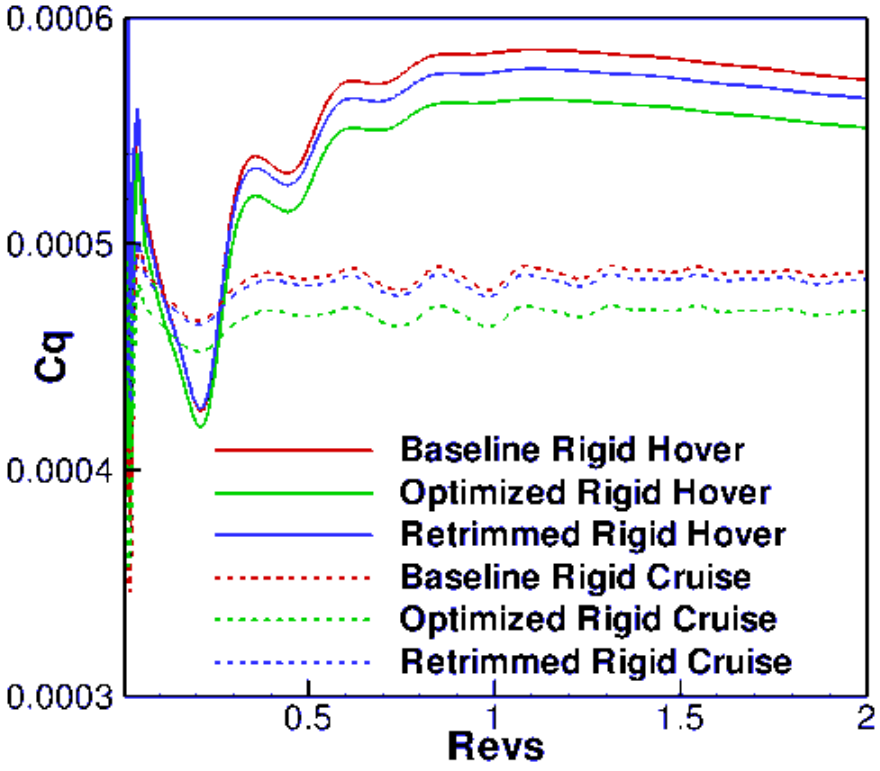

Thrust vs time

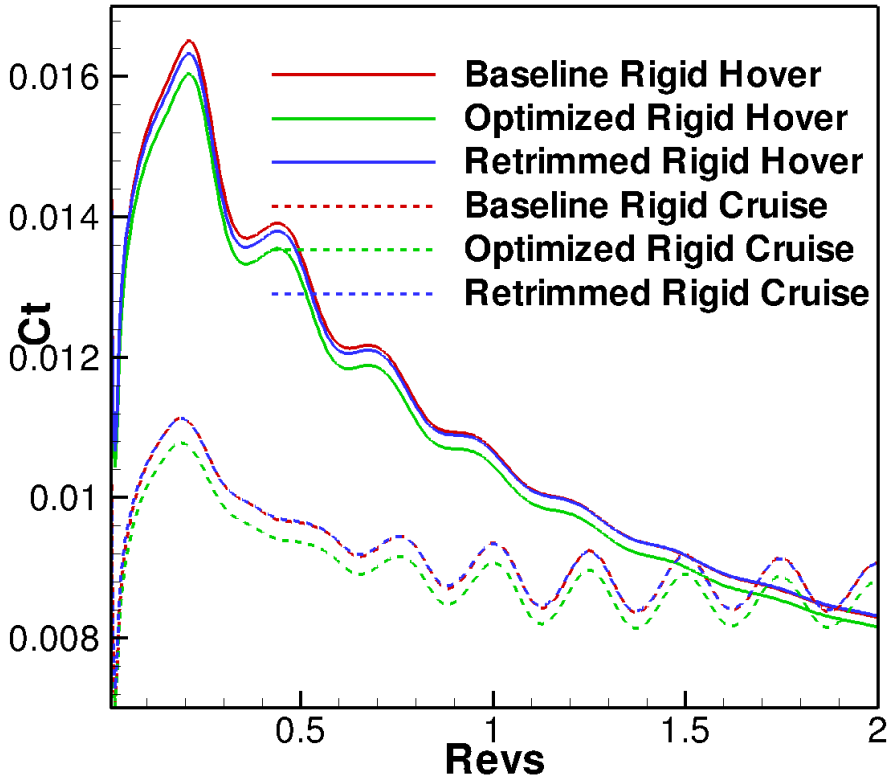

- Trimmed to target thrust, zero moments (~1e-5)
- Overall power reduction w/ shape optimization after retrim: **~1.5**% (hover) and **~0.75**% (cruise)

Rigid Multipoint Optimized Blade Shape (ω_{hover} , ω_{cruise}) = (0.25,0.75)

Baseline

Optimized

Thicker inboard and thinner outboard sections

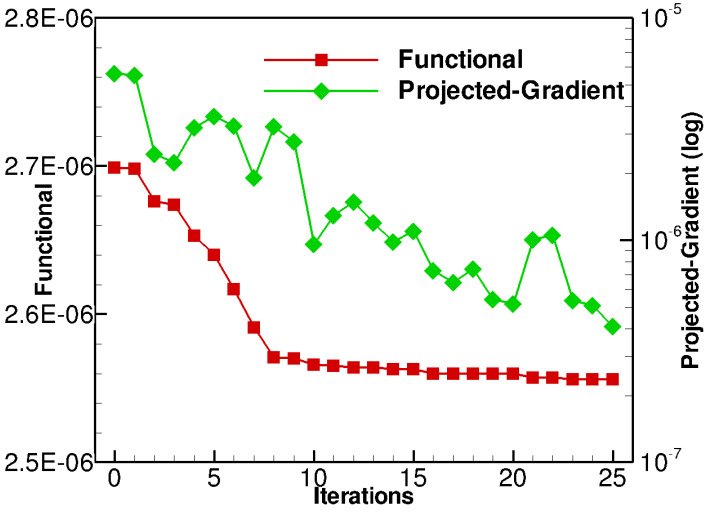

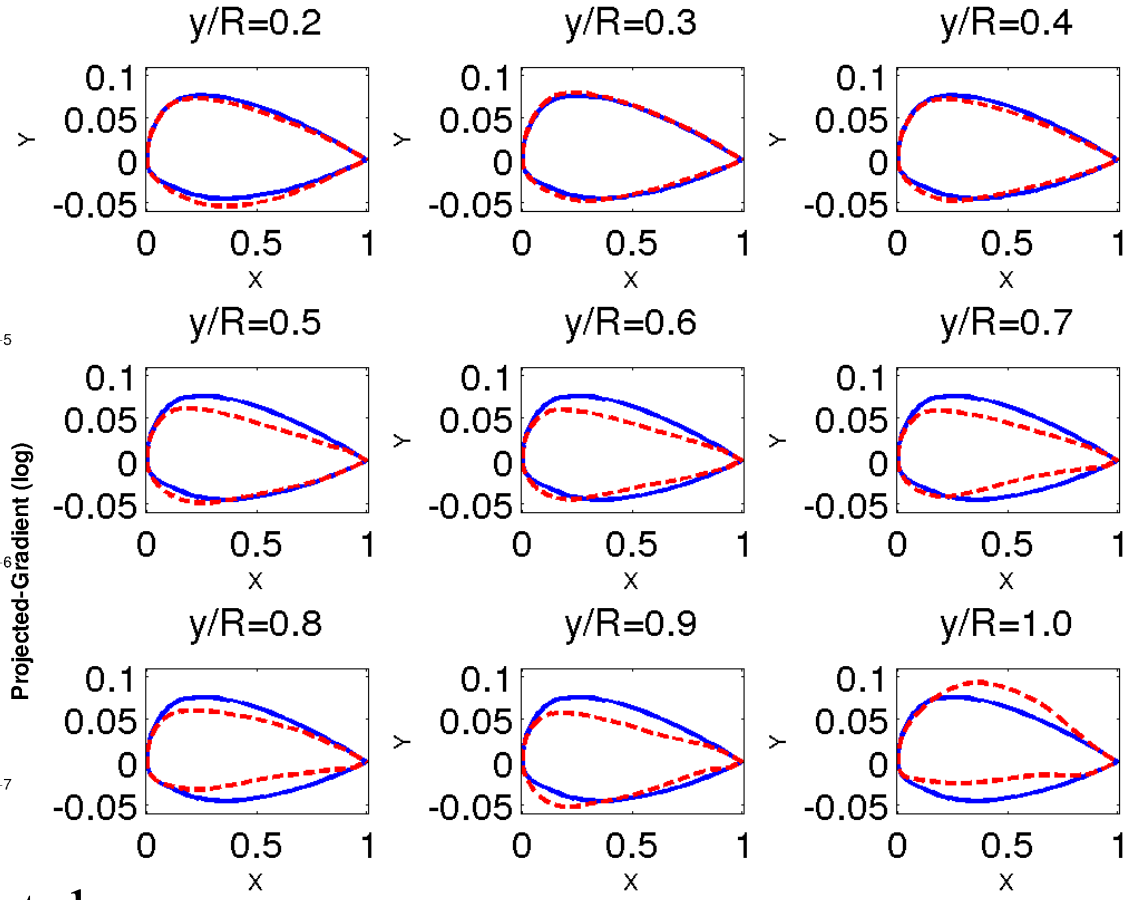

- 1 and ½ order gradient drop, objective converges

Conclusion

- Time dependent tightly coupled CFD/CSD **Analysis** implemented and verified
- Time dependent tangent and adjoint sensitivity for fully coupled CFD/CSD verified on Hart-II rotor in hover **(D=twist)** and forward flight (**D=pitch collective**)
- **Optimized** Hart-II rotor blade in hover/forward flight:
  - Hover: ~5 % power reduction, ~2 % thrust penalty
  - Good trimming demonstrated for Flexible/Rigid blades
  - Flexible/Rigid optimized shape after retrim: ~3% power reduction with same thrust
- Performed multi-point design optimization

Acknowledgements

- Alfred Gessow Rotorcraft Center of Excellence at University of Maryland
- AFOSR STTR Phase I contract FA9550-12C-0048
- University of Wyoming ARCC and NCAR-Wyoming Supercomputer Center

Vehicle Aerodynamic Adjoint Computations

Asitav Mishra, Post-doctoral Scholar

Karthik Duraisamy, Associate Professor

Computational Aerosciences Lab
Department of Aerospace Engineering
University of Michigan, Ann Arbor

Objective

- Adjoint optimization as a feasible tool for (non-aerospace) vehicle shape optimization
  - Surface sensitivities: mesh dependence
  - Verify adjoint sensitivities car geometries
- Results
  - Ahmed Body
  - DrivAer Geometry

The Adjoint Method

Given functional $f(\alpha, U) \;\; subject \;\; to \;\; R(\alpha, U) = 0$

How to compute

$$\frac{df}{d\alpha_i} = \frac{\partial f}{\partial \alpha_i} + \frac{\partial f}{\partial U}\frac{dU}{d\alpha_i}$$

Adjoint method

$$\begin{aligned}\frac{df}{d\alpha_i} &= \frac{\partial f}{\partial \alpha_i} + \frac{\partial f}{\partial U}\frac{dU}{d\alpha_i} + \Psi^T\left[\frac{\partial R}{\partial \alpha_i} + \frac{\partial R}{\partial U}\frac{dU}{d\alpha_i}\right] \\ &= \frac{\partial f}{\partial \alpha_i} + \Psi^T\frac{\partial R}{\partial \alpha_i}\end{aligned}$$

Adjoint Equation

$$if \quad \left[\frac{\partial R}{\partial U}\right]^T \Psi = -\left[\frac{\partial f}{\partial U}\right]^T$$

Adjoint equations are versatile and allow us to estimate functional errors, enable goal oriented mesh adaptation and provide functional sensitivities at low cost.

Surface Sensitivity Adjoint Formulation

Flow and Mesh State:

$$\mathbf{G}(\mathbf{x}, \mathbf{x_s}) = 0$$
$$\mathbf{R}(\mathbf{U}, \mathbf{x}) = 0$$

RHS is obtained from forward residual equations for **G**, **R**.
Adjoint Sensitivity

$$\frac{dCd}{d\mathbf{x_s}} = \begin{bmatrix} \frac{\partial Cd}{\partial \mathbf{x}} & \frac{\partial Cd}{\partial \mathbf{U}} \end{bmatrix} \begin{bmatrix} \frac{\partial \mathbf{x}}{\partial \mathbf{x_s}} \\ \frac{\partial \mathbf{U}}{\partial \mathbf{x_s}} \end{bmatrix}$$

Adjoint RHS obtained from adjoint residual of **G**, **R**

$$\frac{dCd^T}{d\mathbf{x_s}} = \frac{\partial Cd^T}{\partial \mathbf{x_s}} + \begin{bmatrix} -\frac{\partial \mathbf{G}^T}{\partial \mathbf{x_s}} & 0 \end{bmatrix} \begin{bmatrix} \Lambda_\mathbf{x} \\ \Lambda_\mathbf{u} \end{bmatrix}$$

Adjoint Formulation continued…

Forward residual equations:

$$\begin{bmatrix} \frac{\partial \mathbf{G}}{\partial \mathbf{X}} & 0 \\ \frac{\partial \mathbf{R}}{\partial \mathbf{X}} & \frac{\partial \mathbf{R}}{\partial \mathbf{U}} \end{bmatrix} \begin{bmatrix} \frac{\partial \mathbf{X}}{\partial \mathbf{X_S}} \\ \frac{\partial \mathbf{U}}{\partial \mathbf{X_S}} \end{bmatrix} = \begin{bmatrix} -\frac{\partial \mathbf{G}}{\partial \mathbf{X_S}} \\ 0 \end{bmatrix}$$

Adjoint residual equations:

$$\begin{bmatrix} \frac{\partial \mathbf{G}}{\partial \mathbf{X}}^T & \frac{\partial \mathbf{R}}{\partial \mathbf{X}}^T \\ 0 & \frac{\partial \mathbf{R}}{\partial \mathbf{U}}^T \end{bmatrix} \begin{bmatrix} \Lambda_{\mathbf{X}} \\ \Lambda_{\mathbf{U}} \end{bmatrix} = \begin{bmatrix} \frac{\partial Cd}{\partial \mathbf{X}}^T \\ \frac{\partial Cd}{\partial \mathbf{U}}^T \end{bmatrix}$$

Ahmed Body Flow

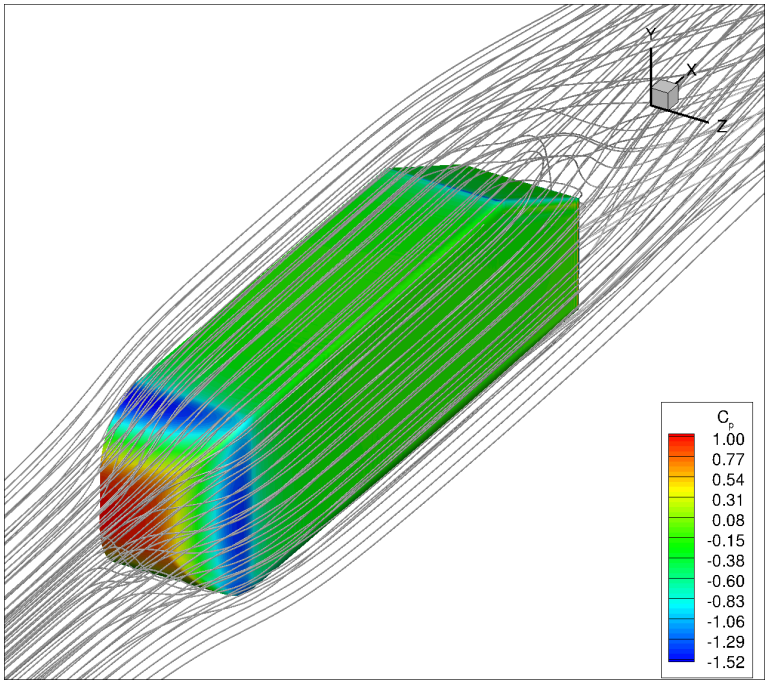

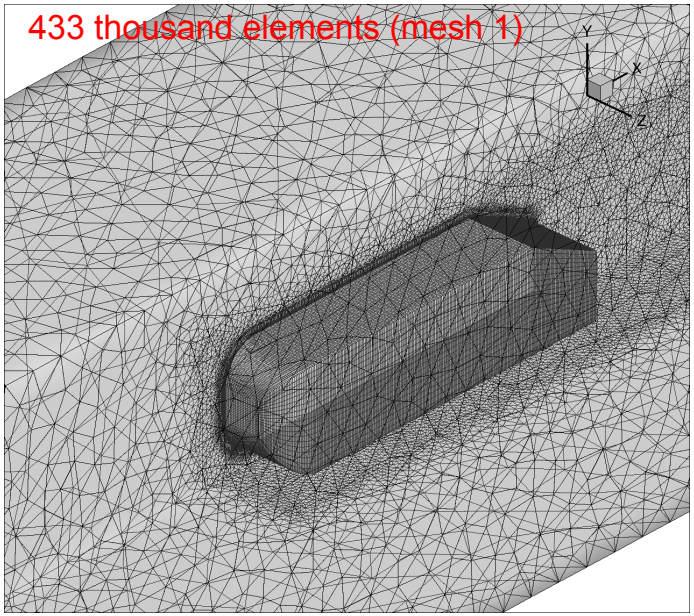

Flow viz and surface pressure: Cd=0.275
(Exp Cd ~ 0.25)

- Ahmed body at U=60 m/s, zero slant flow
- JST 2nd order flow, 1st order Turbulence

Flow convergence history

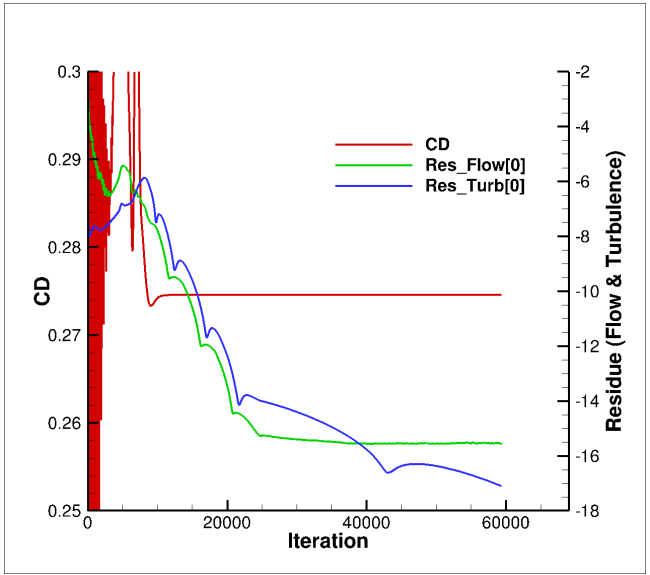

Ahmed Body Two Meshes

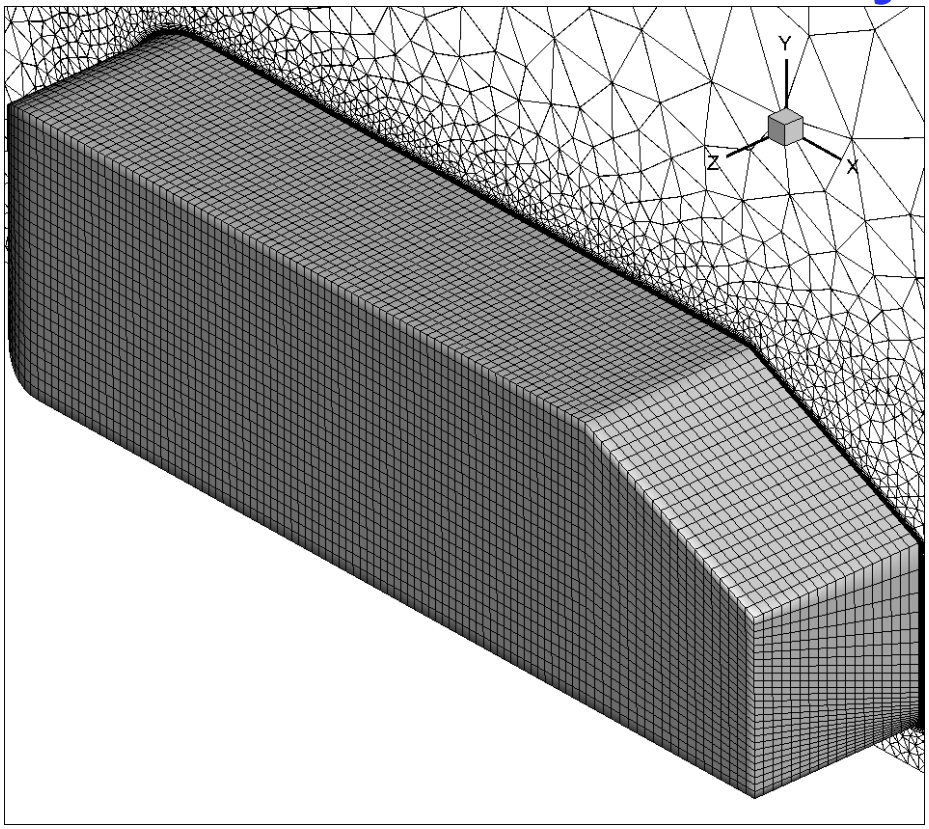

Mesh 1 (202k Nodes)

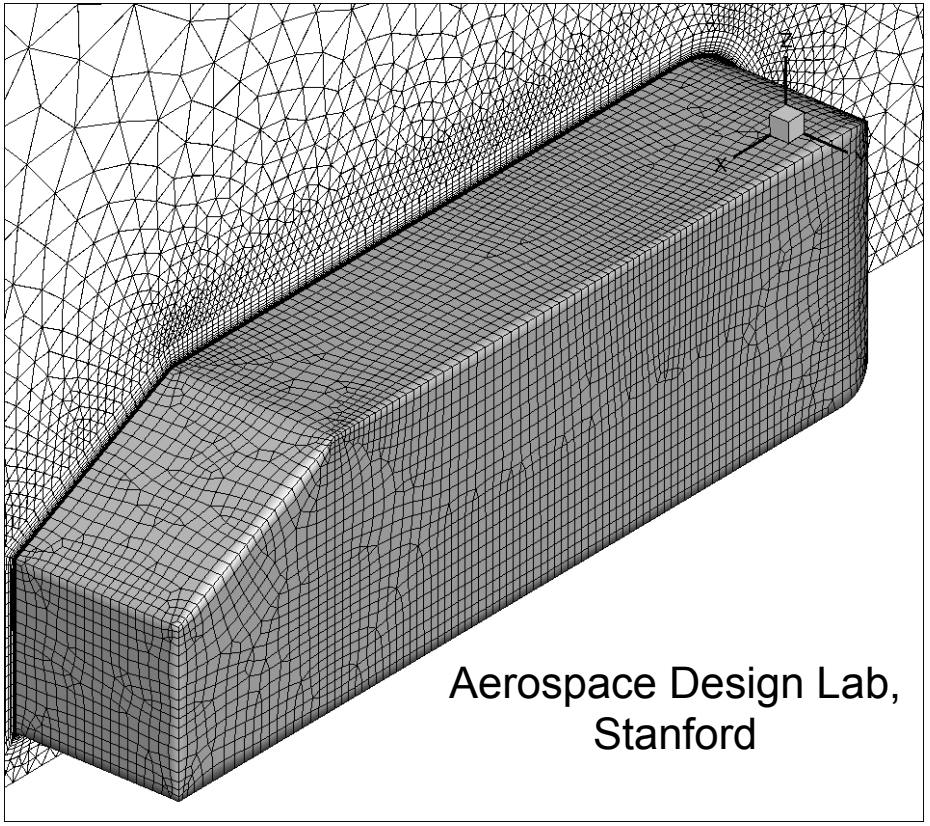

Mesh 2 (250k Nodes)

Ahmed Body Drag Surface Sensitivity

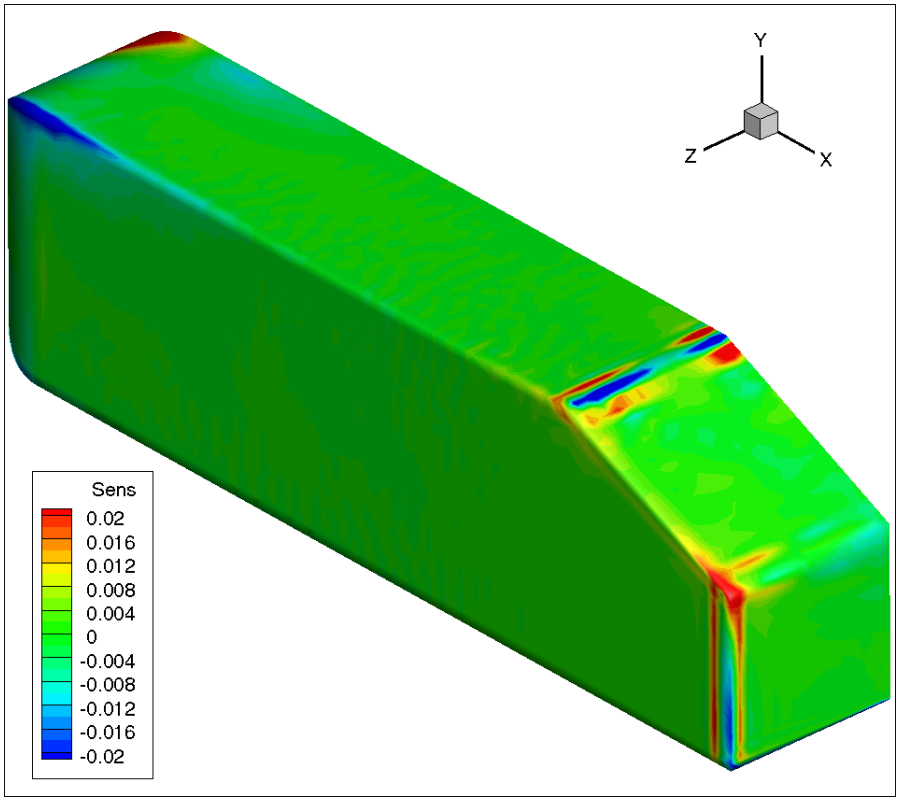

Mesh 1 (202k Nodes)

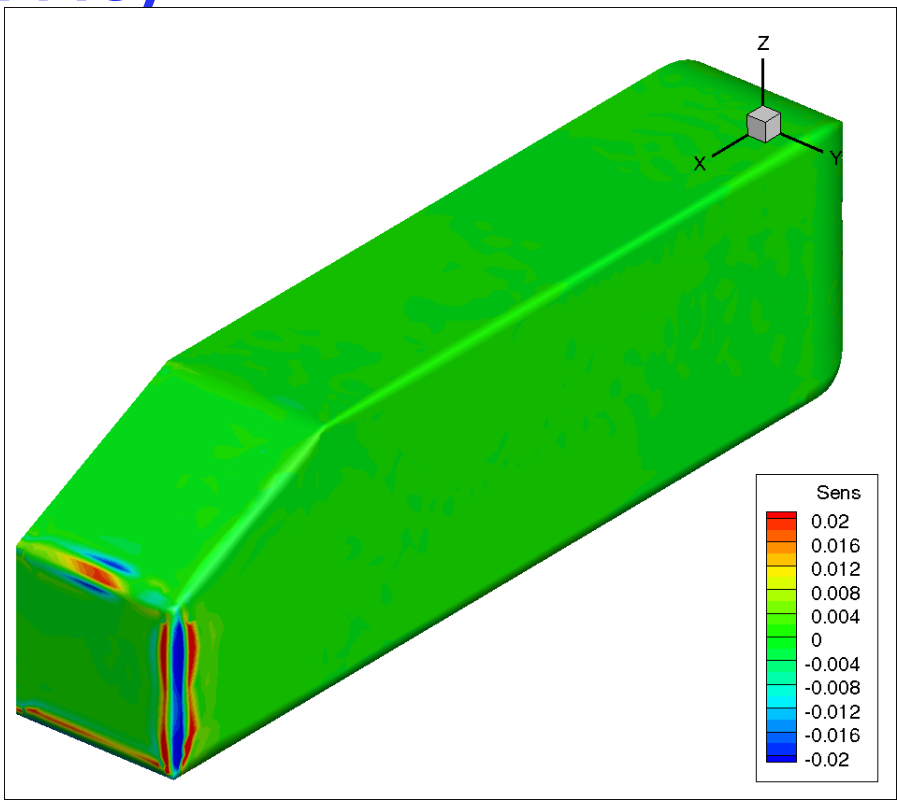

Mesh 2 (250k Nodes)

Discrete solution is mesh sensitive.

Ahmed Body FFD Deformation

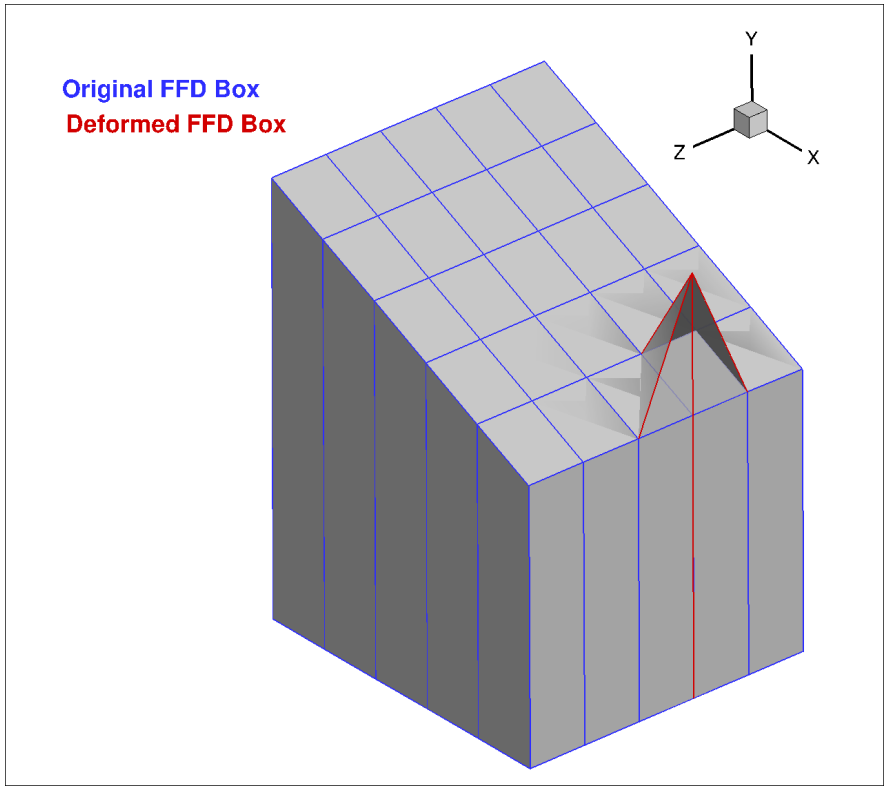

FFD deformation

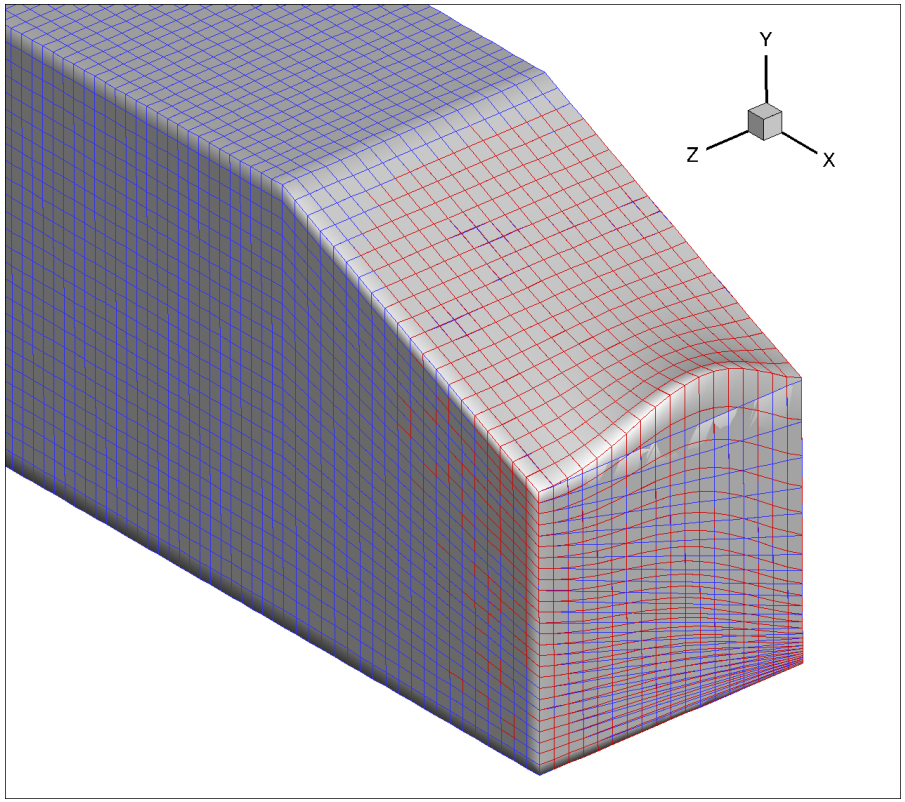

Mesh deformation due to FFD

Ahmed Body Discrete Adjoint FFD Verification: mesh1

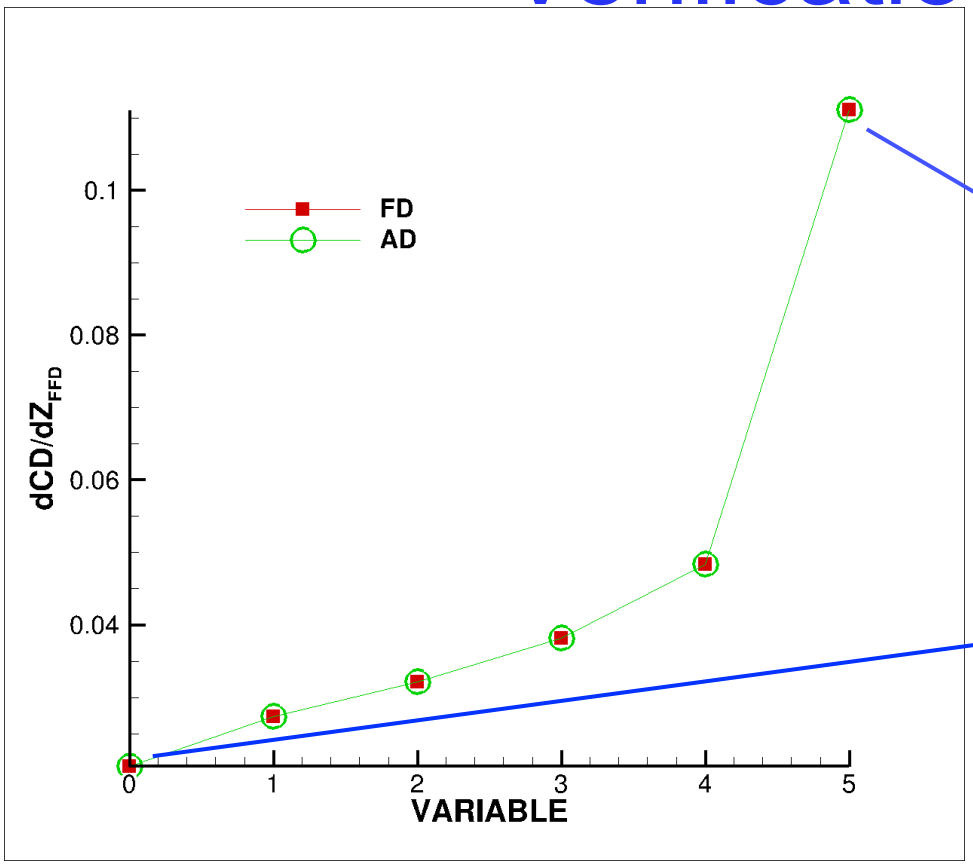

Drag surface sensitivity

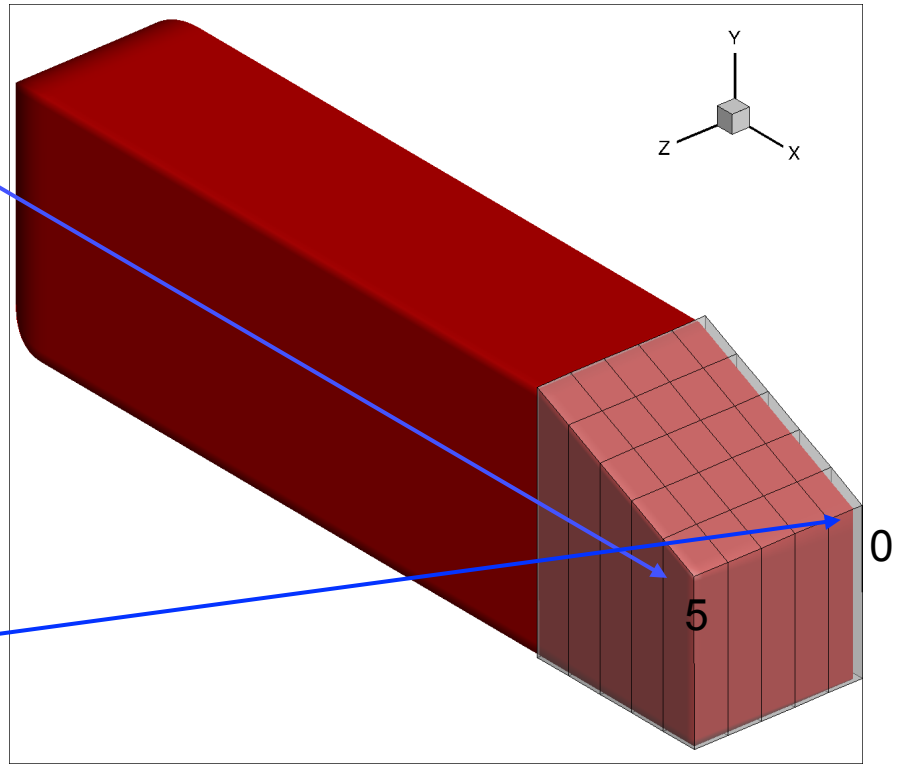

FFD Box

Discrete surface sensitivity verified.

Ahmed Body Discrete Adjoint FFD Verification: mesh2

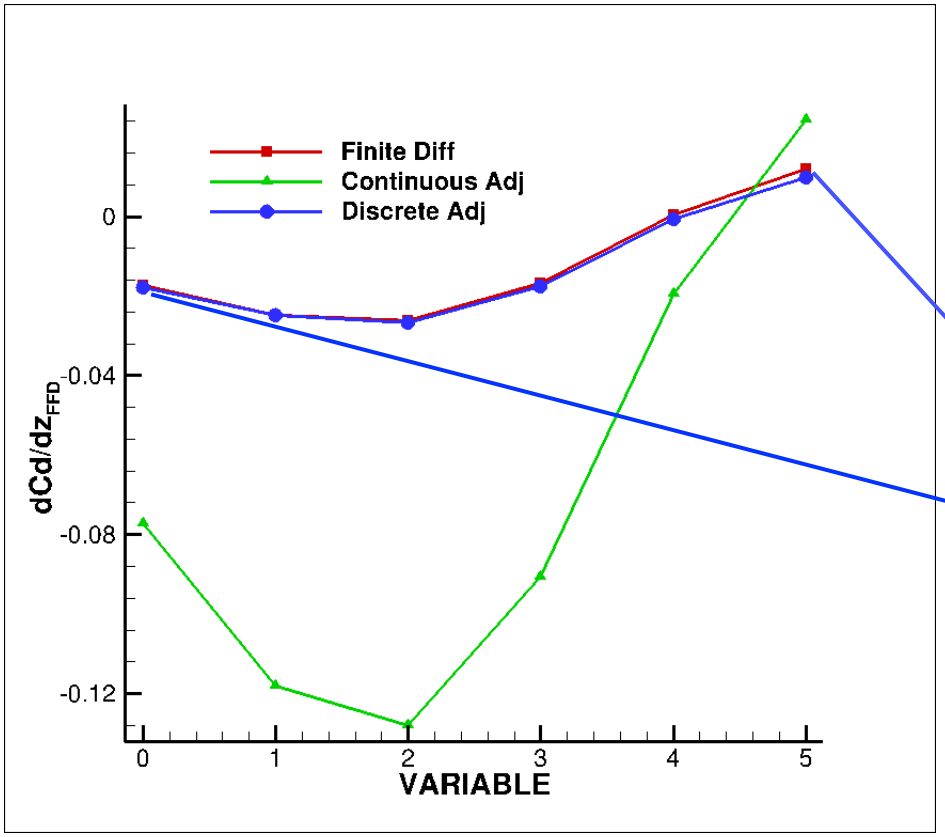

Drag surface sensitivity

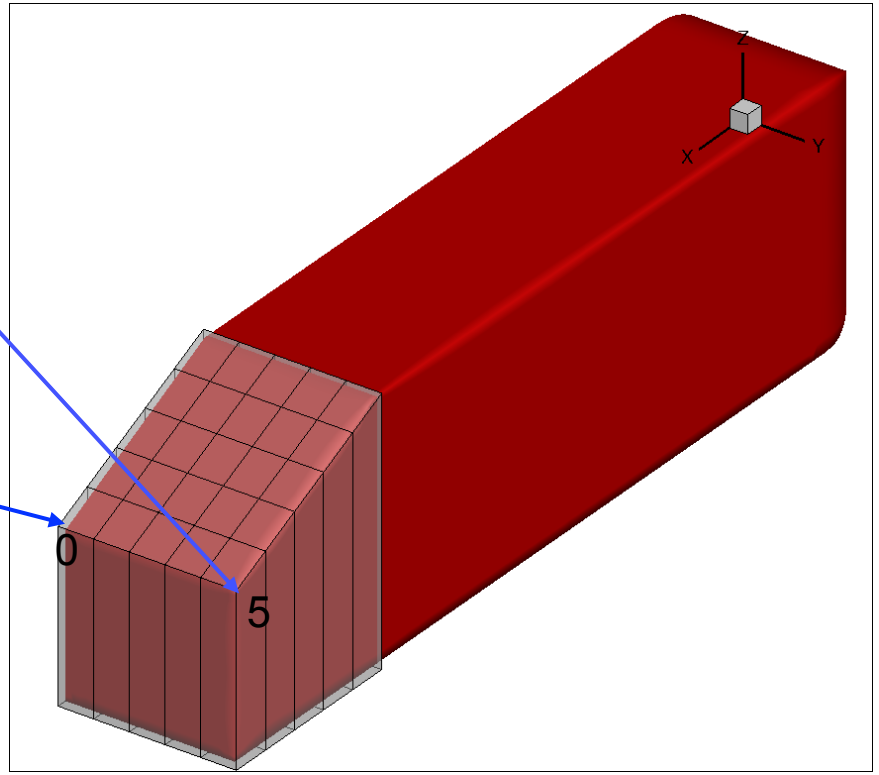

FFD Box

Discrete surface sensitivity verified.

DrivAer Flow Solution

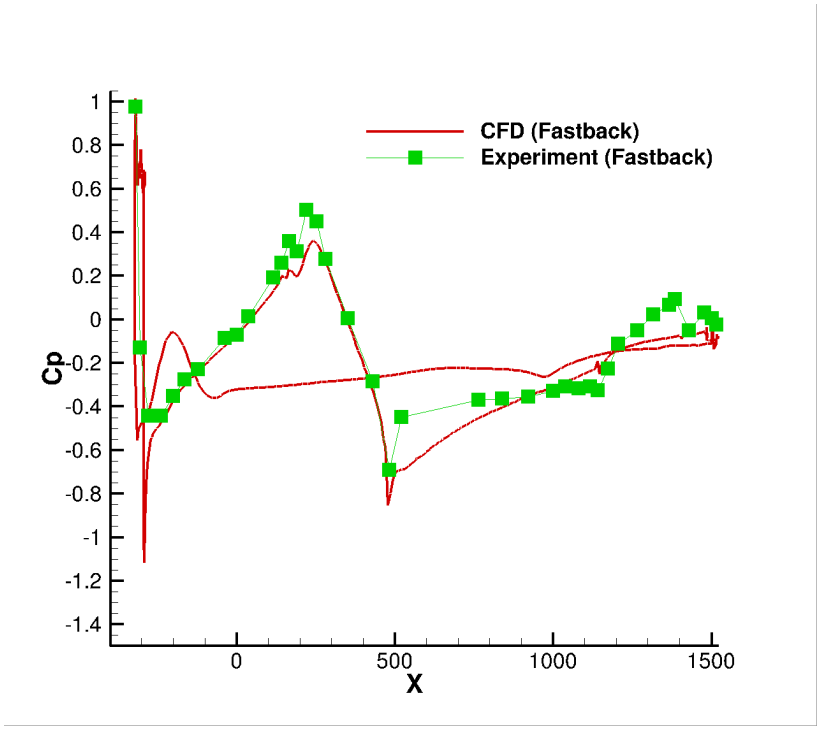

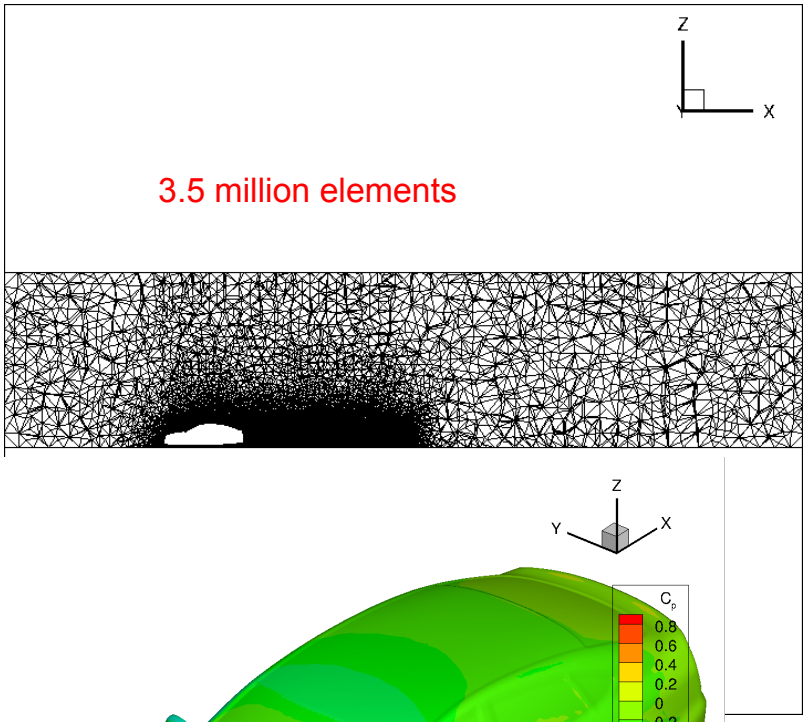

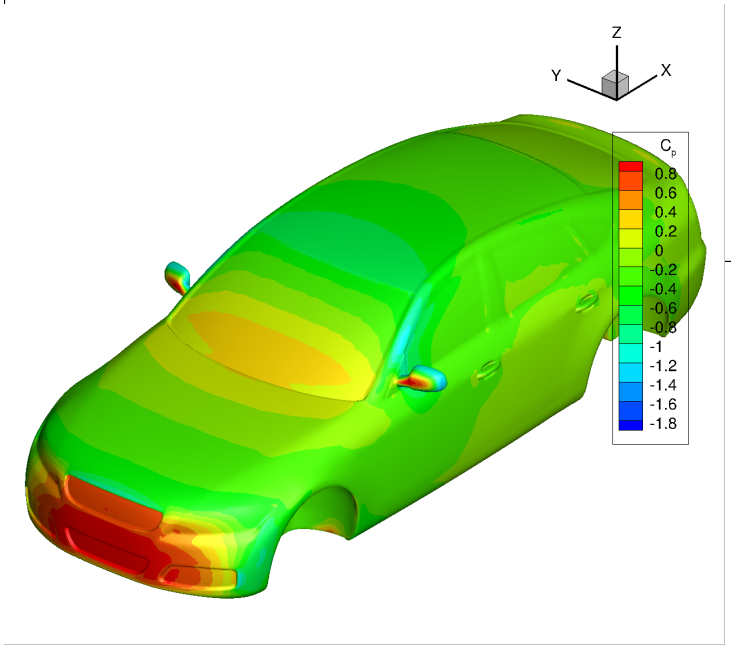

Discrete Adjoint Drag Surface Sensitivity

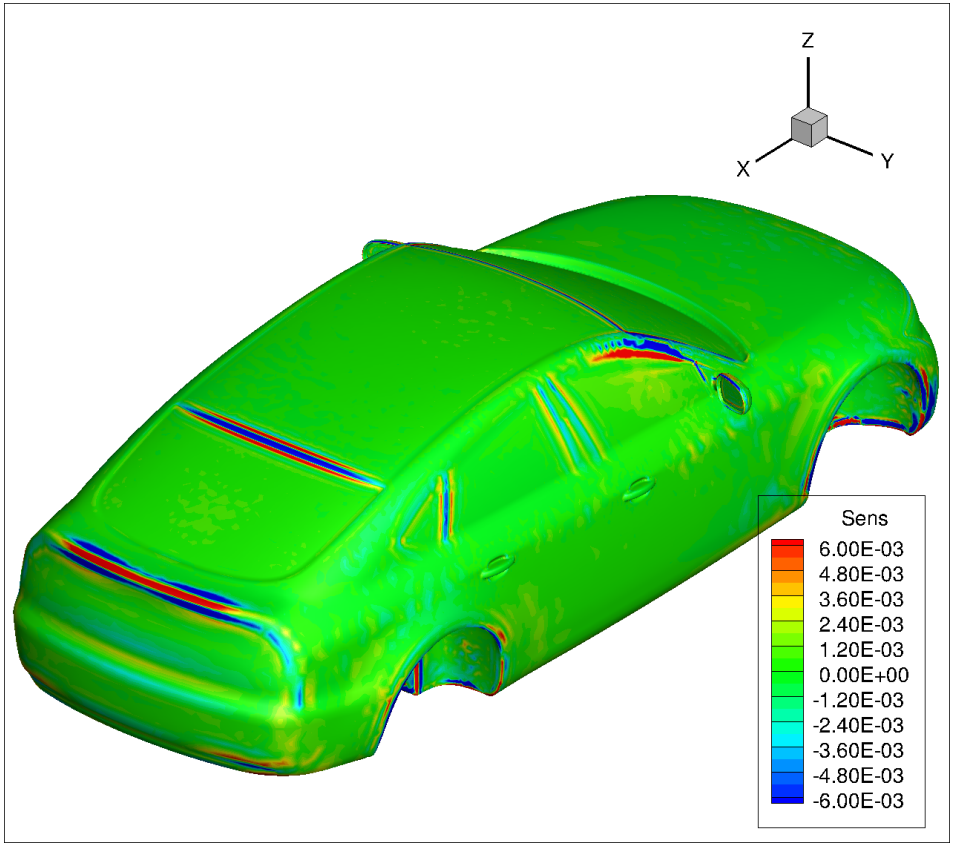

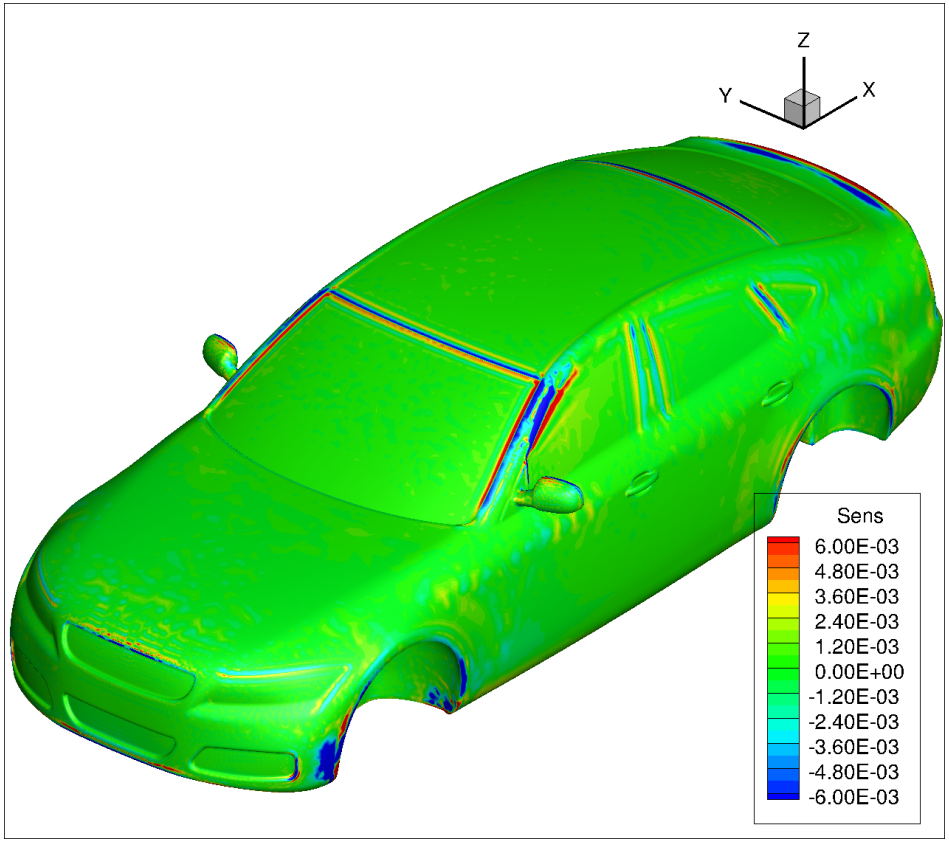

Surface sensitivity

If we want to see the noise

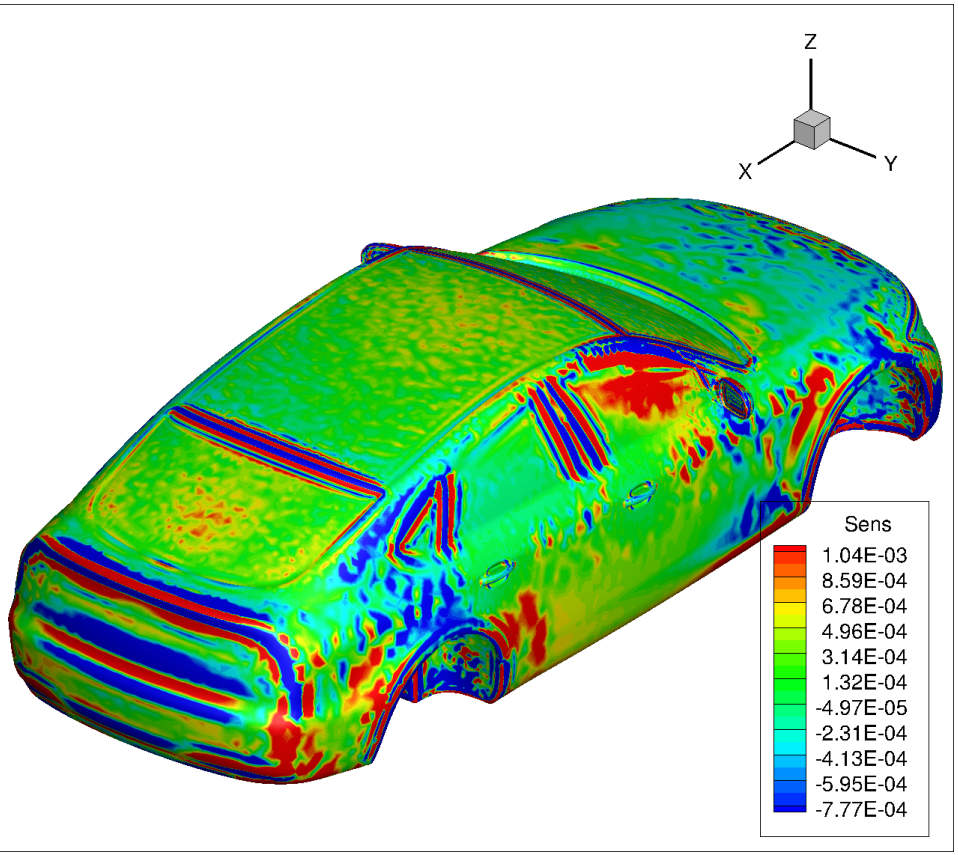

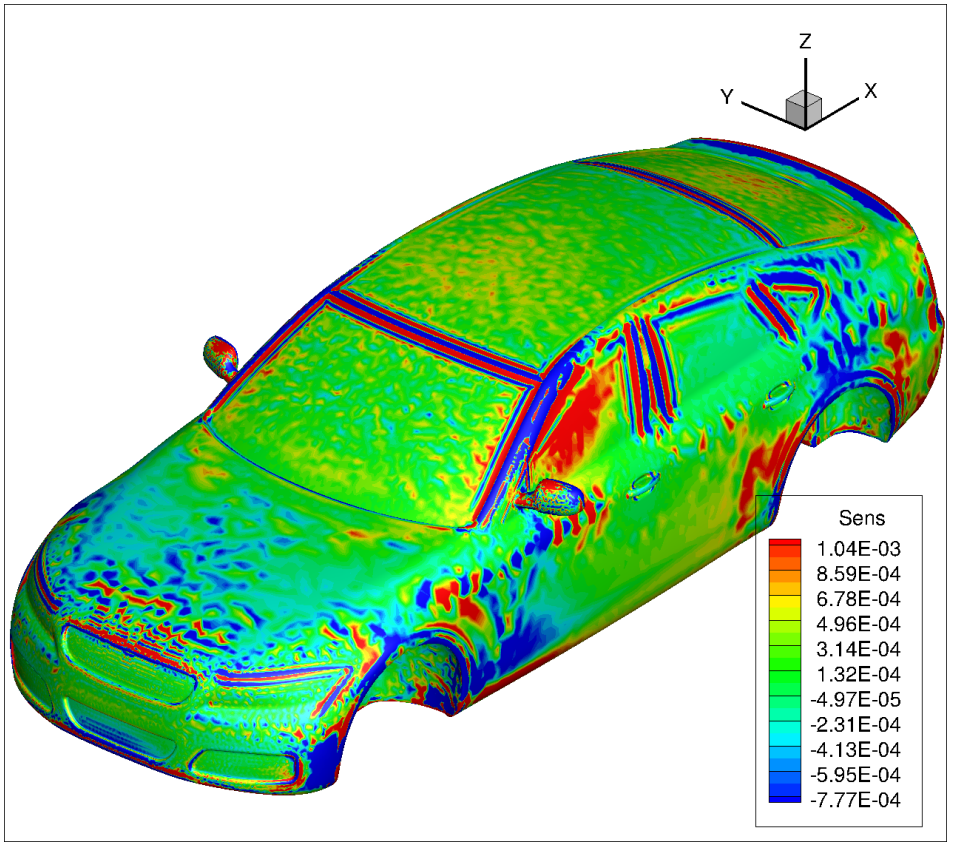

Noise in low sensitivity regions

Discrete Adjoint & FFD

3.5 million elements

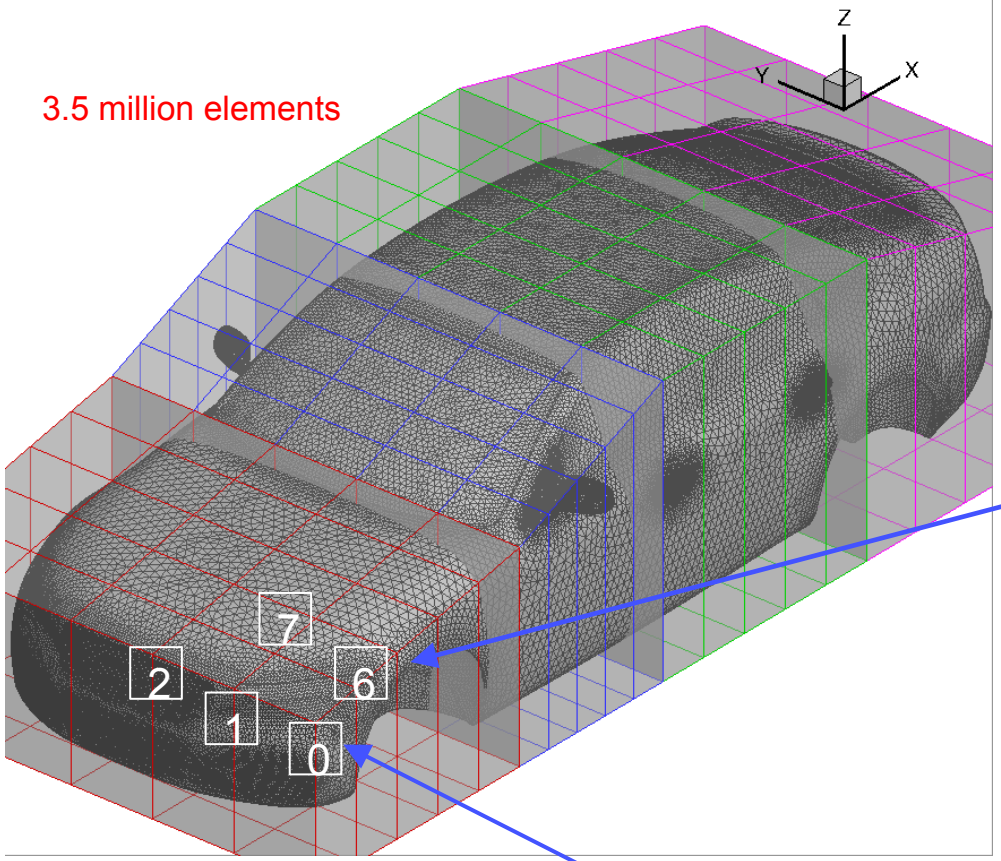

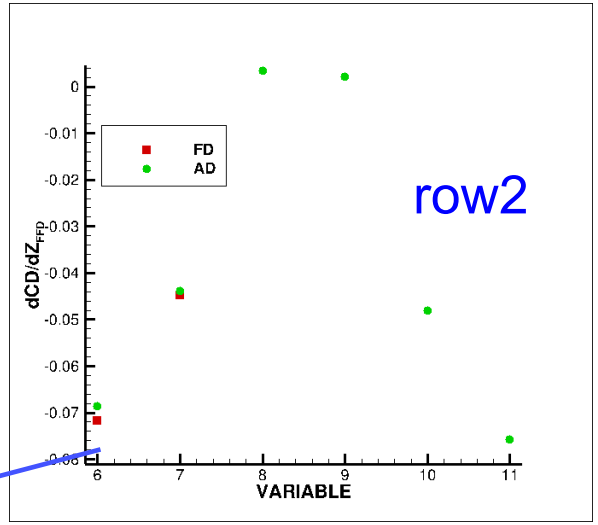

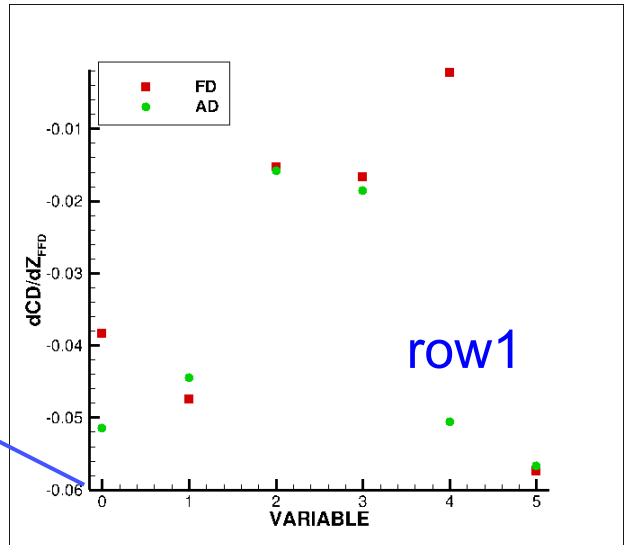

Summary

- Methods of studying sensitivities
- ➔ Surface sensitivities (too local)
- ➔ Free-form deformation boxes (best approach)

- Ahmed body
- ➔ Different meshes (gradients sensitive to mesh)
- ➔ FFD & surface sensitivities

- DrivAer Geometry
- ➔ FFD & surface sensitivities